

Matthew Thomas Ferreira

**Análise de como a produção e atividade de
PGD₂ afetam linhagens de glioma**

Dissertação apresentada ao Programa de Pós-Graduação em Biologia Celular e Tecidual do Instituto de Ciências Biomédicas da Universidade de São Paulo, para obtenção do Título de Mestre em Ciências.

São Paulo
2014

Matthew Thomas Ferreira

**Análise de como a produção e atividade de PGD₂ afetam
linhagens de glioma**

Dissertação apresentada ao Programa de Pós-Graduação em Biologia Celular e Tecidual do Instituto de Ciências Biomédicas da Universidade de São Paulo, para obtenção do Título de Mestre em Ciências.

Área de concentração: Biologia Celular e Tecidual

Orientadora: Profa. Dra. Alison Colquhoun

Versão original

São Paulo
2014

DADOS DE CATALOGAÇÃO NA PUBLICAÇÃO (CIP)
Serviço de Biblioteca e Informação Biomédica do
Instituto de Ciências Biomédicas da Universidade de São Paulo

© reprodução total

Ferreira, Matthew Thomas.

Análise de como a produção e a atividade de PGD2 afetam linhagens de gliomas / Matthew Thomas Ferreira. -- São Paulo, 2014.

Orientador: Profa. Dra. Alison Colquhoun.

Dissertação (Mestrado) – Universidade de São Paulo. Instituto de Ciências Biomédicas. Departamento de Biologia Celular e do Desenvolvimento. Área de concentração: Biologia Celular e Tecidual. Linha de pesquisa: Metabolismo de tumores.

Versão do título para o inglês: Analysis of the how the production and activity of PGD2 affects glioma cell lines.

1. Glioma-análise 2. Apoptose 3. Imunohistoquímicas 4. Prostaglandina sintase 5. Linhagem celular I. Colquhoun, Profa. Dra. Alison II. Universidade de São Paulo. Instituto de Ciências Biomédicas. Programa de Pós-Graduação em Biologia Celular e Tecidual III. Título.

ICB/SBIB0196/2014

UNIVERSIDADE DE SÃO PAULO
INSTITUTO DE CIÊNCIAS BIOMÉDICAS

Candidato(a): Matthew Thomas Ferreira.

Título da Dissertação: Análise de como a produção e a atividade de PGD2 afetam linhagens de gliomas.

Orientador(a): Profa Dra. Alison Colquhoun.

A Comissão Julgadora dos trabalhos de Defesa da **Dissertação de Mestrado**,
em sessão pública realizada a/...../....., considerou

Aprovado(a)

Reprovado(a)

Examinador(a): Assinatura:
Nome:
Instituição:

Examinador(a): Assinatura:
Nome:
Instituição:

Presidente: Assinatura:
Nome:
Instituição:



UNIVERSIDADE DE SÃO PAULO
INSTITUTO DE CIÊNCIAS BIOMÉDICAS

Cidade Universitária "Armando de Sales Oliveira"
Av. Prof. Lúcio Prestes, 2478 - CEP. 05508-000 São Paulo, SP - Brasil
Telefone: (55) (11) 3091-7733 - telex: (55) (11) 3091-0495
e-mail: cep@icb.usp.br

Comitê de Ética em Pesquisa

CERTIFICADO DE ISENÇÃO

Certificamos que o Protocolo CEP-ICB N° 567/12 referente ao projeto intitulado: *"Análise de como a produção e a atividade de PGD2 competem com a ação da PGE2 em glioblastoma multiforme"* sob a responsabilidade de Matthew Thomas Ferreira, foi analisado na presente data pela CEUA - COMISSÃO DE ÉTICA NO USO DE ANIMAIS e pela CEPSh- COMISSÃO DE ÉTICA EM PESQUISA COM SERES HUMANOS, tendo sido deliberado que o referido projeto não utilizará animais que estejam sob a égide da lei 11.794 de 8 de outubro de 2008, nem envolverá procedimentos regulados pela Resolução CONEP n°196 de 1996.

São Paulo, 30 de outubro de 2012.

PROF. DR. WOTHAN TAVARES DE LIMA
Coordenador da CEUA - ICB/USP

PROF. DR. PAULO M.A. ZANOTTO
Coordenador da CEPsh - ICB/USP

ACKNOWLEDGEMENTS

Firstly, I would like to thank my God for putting me in this program and for keeping me, sustaining me, and guiding me until the end. I would like to thank my wife Marcela for all of her support, patience, and prayers. I would like to thank Professor Dr. Alison Colquhoun for her guidance and patience. I also thank Marley Januário da Silva for her support and pleasant attitude. I thank Renata Gomes, Felipe de Costa Souza and Fábio Feitoza for their amazing level of support, care, and willingness to help me whenever I needed. I also give a special thanks to Tatiana Emy de Freitas for being a faithful friend in keeping me encouraged to move forward. Thank you CAPES for supporting me during this project.

ABSTRACT

Ferreira MT. Analysis of how the production and activity of PGD₂ affects glioma cell lines. [Masters thesis (Cell and Tissue Biology)]. São Paulo: Instituto de Ciências Biomédicas, Universidade de São Paulo; 2014.

The World Health Organization classifies glioblastoma (GBM) as a type IV astrocytoma, making it one of the most fatal tumors that exists. Despite the advances in chemotherapy, surgery, and radiation treatments that improve a patient's length of survival, the overall trajectory of the disease remains unchanged. It has been shown that GBM cells produce significant levels of prostaglandins, including prostaglandin D₂ (PGD₂). PGD₂ possesses pro- and anti-tumorigenic properties. Hence, a more complete understanding of PGD₂ activity in GBM could yield more effective treatments against GBM. Through techniques like RT-PCR, immunohistochemistry, and HPLC tandem mass spectrometry, we were able to confirm the capacity for synthesis of PGD₂ in GBM cell lines. We treated GBM cell lines with various concentrations of exogenous PGD₂ over 72 hours and observed its effects on cell count, apoptosis, mitosis and viability. Our results suggest that PGD₂ possesses contradictory functions in GBM depending on concentration (μM PGD₂ vs. nM PGD₂) and receptor activation.

Keywords: Glioblastoma. Prostaglandin. Eicosanoids. Cancer. Opposing roles. PGD₂. PGE₂.

RESUMO

Ferreira MT. Análise de como a produção e atividade de PGD₂ afetam linhagens de glioma. [dissertação (Mestrado em Biologia Celular e Tecidual)]. São Paulo: Instituto de Ciências Biomédicas, Universidade de São Paulo; 2014.

A Organização Mundial de Saúde classifica glioblastoma (GBM) como um astrocitoma tipo IV, fazendo uns dos tumores mais fatais que existe. Apesar dos avanços em quimioterapia, cirurgia e radioterapia que melhoram a longevidade de sobrevivência, a trajetória geral da doença permanece imutável. Tem sido demonstrado que células de GBM produzem níveis significativos de prostaglandinas, incluindo prostaglandina D2 (PGD₂). PGD₂ possui propriedades pro- e anti-tumorigênicas. Então, um entendimento mais completo da atividade de PGD₂ em GBM pode gerar tratamentos mais efetivos. Através de técnicas como RT-PCR, imunohistoquímica e HPLC espectrometria de massas em tandem, conseguimos confirmar capacidade de síntese de PGD₂ em linhagens de GBM. Tratamos linhagens de GBM com concentrações variáveis de PGD₂ exógeno durante 72 horas e observamos seus efeitos na contagem de células, apoptose, mitose e viabilidade. Nossos resultados sugerem que PGD₂ possui funções opostas em GBM dependendo da concentração (μ M PGD₂ vs. nM PGD₂) e ativação de receptores.

Palavras-chave: Glioblastoma. Prostaglandina. Eicosanoides. Câncer. Papeis opostos. PGD₂. PGE₂.

LIST OF FIGURES

Figure 1.1 – Biochemical Pathways influenced by PGD ₂ and PGE ₂	18
Figure 3.1 – Growth Curve A-172 Cell Line.....	21
Figure 3.2 – Growth Curve U-138MG Cell Line.....	21
Figure 3.3 – Growth Curve U-251MG Cell Line.....	22
Figure 3.4 – Growth Curve U-87MG Cell Line.....	22
Figure 3.5 – Growth Curve T-98G Cell Line.....	23
Figure 4.1 – Immunohistochemistry for the U-87MG Cell Line.....	36
Figure 4.2 – HP-LC Tandem Mass Spectrometry in the U-251MG Cell Line.....	38
Figure 4.3 – HP-LC Tandem Mass Spectrometry in the U-87MG Cell Line.....	39
Figure 4.4 – U-251MG Cell Line and Physiological PGD ₂ Treatment.....	41
Figure 4.5 – U-251MG Cell Line and PGE ₂ Treatment.....	42
Figure 4.6 – A-172 Cell Line and Physiological PGD ₂ Treatment.....	43
Figure 4.7 – A-172 Cell Line and PGE ₂ Treatment.....	44
Figure 4.8 – A-172 Cell Line and Supraphysiological PGD ₂ Treatment.....	45
Figure 4.9 – U-87MG Cell Line and Supraphysiological PGD ₂ Treatment.....	46
Figure 4.10 – U-251MG Cell Line and Supraphysiological PGD ₂ Treatment.....	47
Figure 4.11 – Viability of U-251MG Cell Line with PGD ₂	49
Figure 4.12 – Viability of A-172 Cell Line with PGD ₂	50
Figure 4.13 – Viability of U-87MG Cell Line with PGD ₂	51
Figure 4.14 – Apoptotic Responses to PGD ₂	53
Figure 4.15 – Mitotic Responses to PGD ₂	53

LIST OF TABLES

TABLE 3.1 – Primer Sequences and Annealing Temperatures.....	25
TABLE 4.1 – RT-PCR Results.....	32
TABLE 4.2 – Summary of RT-PCR Results.....	34
TABLE 4.3 – Summary of Immunohistochemistry Results.....	37
TABLE 4.4 – Hoechst staining of cells in UV light.....	54
TABLE 5.1 – Summary of Human Protein Atlas Findings.....	60

LIST OF ACRONYMS

CNS – Central Nervous System
GBM – Glioblastoma
EMT – epithelial-to-mesenchymal transition
AA – arachidonic acid
PGG₂ – prostaglandin G2
COX – cyclooxygenase
PGH₂ – prostaglandin H2
PGE₂ – prostaglandin E2
PGD₂ – prostaglandin D2
PGF₂ – prostaglandin F2
PGJ₂ – prostaglandin J2
TXA₂ – thromboxane A2
MRP-4 – multidrug resistance protein 4
PGT – prostaglandin transporter
mPGES – micosomal prostaglandin E synthase
cPGES – cytosolic prostaglandin E synthase
EP – prostaglandin E receptor
PKC – protein kinase C
PKA – protein kinase A
AC – adenylate cyclase
cAMP – cyclic adenosine monophosphate
Kd – dissociation constant
Ki – binding constant
NGF – nerve growth factor
BDNF – brain-derived neurotrophic factor
GST – gluthione S-transferase
GSH – glutathione
DP – prostaglandin D2 receptor
CRTH2 – chemoattractant T-helper 2 receptor
IL – interleukin
PPAR γ – proliferator-activated receptor gamma
TP – thromboxane receptor
TXAS – thromboxane synthase
TNF- α – tumor necrosis factor alpha
PLC – phospholipase C
PIP – Phosphatidylinositol (3,4,5)-trisphosphate
DMEM – Dulbecco's Modified Eagle Medium
FBS – fetal bovine serum
DMSO - dimethylsulfoxide

CONTENTS

1	INTRODUCTION.....	12
1.1	Prostaglandins.....	14
1.2	Prostaglandin E ₂	14
1.3	Prostaglandin D ₂ : Dual Role.....	15
2	OBJECTIVES.....	19
2.1	General Objective.....	19
2.2	Specific Objectives.....	19
3	MATERIALS AND METHODS.....	20
3.1	Cell Culture.....	20
3.2	Growth Curves.....	20
3.3	Total RNA extraction.....	23
3.4	Synthesis of Complementary DNA.....	24
3.5	Primer Design.....	24
3.6	Standardization of Primers by RT-PCR.....	24
3.7	Analysis of mRNA Expression by RT-PCR.....	26
3.8	Cell Line Selection.....	26
3.9	HPLC-MS/MS.....	27
3.10	Dose-Response Curve.....	27
3.11	Immunohistochemical Reactions.....	28
3.12	Viability Test.....	29
3.13	Apoptosis and Mitosis Tests.....	29
3.14	Data Analysis.....	30
4	RESULTS.....	31
4.1	PCR.....	31
4.2	Immunohistochemistry.....	35
4.3	HPLC-MS/MS.....	38
4.4	Dose-Response Curve.....	40
4.5	Viability Test (MTT).....	48
4.6	Apoptosis and Mitosis Reactions.....	52
5	DISCUSSION.....	55
5.1	The Confirmed Presence of the PGD ₂ Synthesis Pathway.....	55
5.2	The Impact of PGD ₂ on Cellular Activity.....	62
6	CONCLUSION.....	65
	REFERENCES.....	67

1 INTRODUCTION

In normal cell division, the cells sometimes suffer genetic mutations that could affect their structures and functions. Many times the cellular repair mechanisms are able to correct the mutation or adapt the cell to the mutation preserving the original function of the cell. If the cell cannot repair enough of the damaged DNA, it enters into apoptosis, or cell death. However, sometimes the cells do not respond to the apoptotic signals and continue to replicate. Once they begin to invade and migrate into other tissues of the body, the cells are considered cancerous. In 1874 the famous surgeons, Sir Jonathan Hutchinson and Campbell Greig De Morgan, believed that cancer started from single origins, and referred to cancer as the rebellion of cells (Grange et al., 2002). Today, as seen in Aktipis and Nesse's review of evolutionary foundations for cancer biology, various stimuli of this cellular "rebellion" have actually been exposed as evolutionary stimuli, such as inflammation (Aktipis and Nesse, 2013). Some of the known causes of cancer vary from genetic mutations to epigenetic changes, and from chronic inflammation to diet and lifestyle risk factors (Wang and Dubois, 2010).

In 2011 Jemal et al., cited that an estimate of 7.6 million people die of cancer every year in the world. The Globocan organization cites that in South America in 2012, 19,865 incidents of brain cancer were diagnosed and 14,812 deaths occurred because of this cancer. In five years they predict that there will be 28,305 incidents of brain cancer in South America. When examining the Americas, Brazil has the highest brain cancer incidence and mortality rate (Ferlay et al., 2013; Jemal et al., 2011). There is a need in this country, as in the rest of the world, to explore more effective treatments in these more aggressive forms of brain cancer.

The brain is composed of nervous tissue. The types of cells that compose the nervous tissue can be classified as neurons and glial cells (neuroglia or glia). Previously, it was assumed that the glial cells only possessed the function of sustaining or insulating the action potential of the neuronal axon. Today a network of pathways and intercellular interactions are being explored because more diversified roles of glial cells are being discovered (Parpura et al., 2012). There are four main types of glial cells: astrocytes, oligodendrocytes, ependymal cells, and microglia. Their various functions are crucial in the operation of the Central Nervous System (CNS),

because they help define brain homeostasis and defend against pathological complications, amongst other activities (Parpura et al., 2012; Pfriederger, 2009).

Astrocytomas are CNS neoplasms in which the principal cell type is resulting from an immortalized astrocyte (Greenberg, 1997). The World Health Organization designates four different grades for astrocytomas. A Grade I astrocytoma is also known as a pilocytic astrocytoma. This low grade tumor is benign and typically possesses clearly defined boundaries making a thorough surgery possible for the patients who tend to be less than twenty years old (Otero et al., 2011). A Grade II astrocytoma, known as a diffuse astrocytoma, is also considered a low-grade astrocytoma because of its lack of significant mitotic activity, vascular proliferation, and necrosis. Unfortunately, because of its ability to spread, this type of astrocytoma complicates the outcome in pediatric patients (Fisher et al., 2008). In adult patients, a diffuse astrocytoma can progress to high-grade astrocytomas (Fausto et al., 2013). If treated before significant progression has occurred, patients may have an overall survival rate of 6 to 8 years. High-grade astrocytomas begin with Grade III astrocytomas, also known as anaplastic astrocytomas. After chemotherapy and surgery, patients have a survival rate of about 2 to 3 years (Rao et al., 2014).

The World Health Organization classifies glioblastoma (GBM) as a type IV astrocytoma, making it one of the most fatal tumors that exists (Louis et al., 2007). GBM is furthered classified as primary or secondary based on clinical and molecular profiling. Primary GBM is the most common consisting of >90% of all GBMs with no evidence of progression from low-grade astrocytomas (Rao et al., 2014). In primary GBM, even after surgical and chemical treatment the life expectancy is still less than 15 months (Ohgaki and Kleihues, 2013; Vauleon et al., 2010). Secondary GBM, in general, results from the progressive malignant transformation of diffuse or anaplastic astrocytomas (Rao et al., 2014).

Despite the advances in chemotherapy, surgery, and radiation treatments that improve a patient's length of survival, the overall trajectory of the disease remains unchanged. There still is a need to investigate the nuances of survival pathways and processes in which GBM advances.

1.1 Prostaglandins

Eicosanoids have been proposed to activate oncogenes and the epithelial-to-mesenchymal transition (EMT), to inhibit tumor suppressor genes, to participate in tumor cell evasion of the immune response, and to initiate angiogenesis. Eicosanoids are bioactive lipids synthesized by cyclooxygenase enzymes from arachidonic acid (AA) (Wang and Dubois, 2010). AA is the most common substrate used in eicosanoid synthesis (Youdim et al., 2000). Phospholipase A₂ releases AA from the membrane-bound phospholipids. AA is then metabolized to form the intermediate prostaglandin G₂ (PGG₂) by cyclooxygenase enzymes (COX). PGG₂ is then reduced to form prostaglandin H₂ (PGH₂) by PG hydroperoxidase (Tassoni et al., 2008). PGH₂ is then metabolized to form PGD₂, PGE₂, PGF₂, PGI₂ and TXA₂ depending on the presence of certain synthases. After synthesis these products are released by multidrug resistance protein 4 (MRP-4) and/or they are taken up into cells by prostaglandin transporter (PGT) (Caterina and Basta, 2001; Sassi et al., 2008). These bioactive lipids, or prostaglandins, produced serve as signaling molecules that participate in diverse physiological and pathological functions in the brain (Sang and Chen, 2006).

GBMs are characterized by high cellular ability to proliferate, invade and migrate. These malignant glial cells can also evade the immune system response, inhibit apoptosis and stimulate angiogenesis (Nathoo et al., 2004). Hanahan and Weinberg define the hallmarks of cancer characteristics as proliferative signaling, evading growth suppressors, resisting cell death, enabling replicative immortality, inducing angiogenesis, and activating invasion and metastasis (Hanahan and Weinberg, 2011). Prostaglandins influence various pathways which produce these observed hallmarks of cancer. It has been shown that GBM cells produce significant levels of prostaglandins (Sawamura, 1990). Therefore, a more complete understanding of prostaglandin activity in GBM could yield more effective treatments against GBM (Tiberiu and Das, 2013).

1.2 Prostaglandin E2

Prostaglandin E₂ (PGE₂) is a pro-inflammatory prostanoid (a chemical messenger) that has a significant role in promoting tumor growth (Nathoo et al., 2004). Nakanishi et al. showed

that the inhibition of the production of endogenous PGE₂ through the genetic deletion of microsomal prostaglandin E synthase 1 (mPGES-1) suppresses intestinal tumorigenesis (Nakanishi et al., 2008). Since this prostanoid is found in abundance in human tumors, there is great need to understand its function. There has been an increase in information concerning the role of PGE₂ signaling in animal models of various cancers, such as GBM, but more investigation is required (Wang and DuBois, 2010).

The cytosolic enzymes responsible for the production of PGE₂ are cytosolic prostaglandin E (c-PGES), microsomal prostaglandin E synthase 1 (m-PGES1) and microsomal prostaglandin E synthase 2 (m-PGES2). These enzymes metabolize PGH₂ to PGE₂ (Jakobsson et al., 2002; Nakatani et al., 2011). It has been shown that c-PGES is more active in the presence of COX-1, m-PGES1 is more active in the presence of COX-2, and m-PGES2 is active in the presence of both COX-1 and COX-2 (Sang and Chen, 2006). Studying the specific roles and actions of these enzymes could offer alternative ways of inhibiting PGE₂ production. Inhibiting PGE₂ synthesis would be an effective target for treatments of GBM or other forms of cancer because of PGE₂'s important role in immunosuppression and tumor growth (Tiberiu and Das, 2013; Hwang et al., 2004).

Prostaglandin E₂ binds and activates four G-protein-coupled receptors commonly referred to as EP1, EP2, EP3, and EP4. When activated, the EP1 receptor activates the protein kinase C (PKC) pathway, which then releases Ca²⁺ ions in the cytoplasm. The EP2 and EP4 receptors are involved in the stimulation of the G-protein (Gs)/ adenylyl cyclase (AC)/ cyclic AMP (cAMP) pathway by stimulating the synthesis of intracellular cAMP which regulates genetic expression. Receptor EP3 is associated with the inhibitory G-protein mechanism (Gi) and reduces the cAMP levels to avoid over-activation of Protein Kinase A (PKA) (which increases lipid production) and other enzymes, as well as the increase of cellular proliferation (Harris et al., 2002). These signaling pathways are activated depending on the amount of PGE₂ present and the binding affinities of each receptor with PGE₂. EP1 has a dissociation factor (K_d) of 20 nM, EP2 has a K_d of 12 nM, EP3 has a K_d of 0.85 nM, and EP4 has a K_d of 1.9 nM (Rundhaug et al., 2011; Kiriya et al., 1997). EP3 and EP4 have the strongest binding affinities for PGE₂.

1.3 Prostaglandin D₂: Dual Role

Prostaglandin D₂ (PGD₂) is a prostanoid that has a role in the pro-/anti-inflammatory response, vasodilation, allergic responses, platelet aggregation, contraction of the airway's smooth muscles, and in other pathways (Keenan and Rangachari, 1991; Sandig et al., 2007). This prostaglandin is one of the most common prostaglandins found in the brain. Its most well-known function is regulating the sleep cycle and promoting the synthesis of nerve growth factor (NGF) and brain-derived neurotrophic factor (BDNF) (Ram et al., 1997; Toyomoto et al., 2004; Zeitzer, 2013). However, its role in glioma progression has not been clearly defined.

The enzymes that synthesize PGD₂ are hematopoietic PGD synthase and lipocalin-type PGD synthase (Sandig et al., 2007). The L-PGDS enzyme also functions to regulate the migration and morphology of glial cells (Lee et al., 2012). Beyond the nervous system, L-PGDS also has an inhibitory effect on the progression of lung, ovarian, colorectal cancer, as well as some types of leukemia (Joo and Sadikot, 2012). H-PGDS is present in various cells of the immune system producing PGD₂ as an allergic and inflammatory mediator. It is also characterized as a member of the glutathione S-transferase (GST) gene family, whose members are known to catalyze the binding of glutathione (GSH) to an electrophilic substrate (Pinzar et al., 2000).

The principal PGD₂ receptors are DP1 and chemoattractant T-helper 2 receptor (CRTH2) also commonly known as DP2. The activation of these receptors produce varying consequences, for example, the activation of DP1 may inhibit production of IFN- γ , inhibit basophil migration, inhibit basophil degranulation, as well as inhibit differentiation of dendritic cells. While examining asthma, Kostenis and Ulven suggested that DP1 may have an overall anti-inflammatory role in the immune system (Kostenis and Ulven, 2006). PGD₂ binds to DP1 with a strong affinity factor (K_i) of 1.7 nM (Yamamoto et al., 2011). Activation of the DP2 receptor can induce migration of Th2 cells, induce interleukin (IL) production, and induce migration and degranulation of eosinophils and basophils. These activities and others designate DP2 as a receptor which stimulates pro-inflammatory responses. PGD₂ has a strong affinity for DP2 with a K_i of 2.4 nM (Sawyer et al., 2002). PGD₂ also can bind to the peroxisome proliferator-activated receptor gamma (PPAR γ). Activation of PPAR γ can cause an increase in eosinophil migration and actin polymerization, inhibit TNF- α , IL-6 and IL-1 β production, inhibit cellular proliferation, and

induce apoptosis (Sandig et al., 2007). There is also evidence in that PGD₂ binds to the thromboxane receptor (TP) in the early phase of the bronchoconstrictor effect (Hamid-Bloomfield et al., 1990). When the enzyme thromboxane synthase was inhibited in rats injected with the U-87MG cell line, thus indirectly limiting TP activation, tumor growth experienced proapoptotic, antiproliferative, and antiangiogenic effects (Schmidt et al., 2010). Binding affinities of PGD₂ to PPAR γ and TP were difficult to find in the available literature.

PGD₂ demonstrates seemingly opposing functions within various systems in the body due to its capacity to influence the pathways that lead to a spectrum of cellular responses. PGD₂ induces a pro-inflammatory condition in the lungs for asthma patients as well as neuroinflammation in mouse models with the myelin sheath degenerative disorder known as Krabbe's disease (Joo and Sadikot, 2012). PGD₂ injection in the skin has also resulted in erythema, edema and induration (Pettipher et al., 2007). However, there is also some developing evidence that supports the idea that PGD₂ has a potentially influential role in anti-tumorigenic activity (Wang and DuBois, 2010). In fact, Honda and Tabuchi showed that PGD₂ could be a potentially useful chemotherapeutic agent to treat malignant gliomas (Honda and Tabuchi, 1986). Evidence of the anti-inflammatory role of PGD₂ and its metabolites were also produced in a study using DP1 knock-out mice. Stimulation of two groups with acute lung inflammation demonstrated that the mice without DP1 could not decrease the inflammation, and the wild-type mice were able to produce more PGD₂ and decrease inflammation (Murata et al., 2013). Also, Wang and Dubois stated in their review that PGD₂ released by stromal cells inhibits *in vitro* prostate tumor cellular growth through a PPAR γ -dependent mechanism (Wang and DuBois, 2010). In light of this growing knowledge base of PGD₂'s varying functions in the immune response, we investigated PGD₂'s influence on GBM, and when possible, compared PGD₂'s influence with PGE₂'s influence. **Figure 1.1** summarizes the pathways considered in this project.

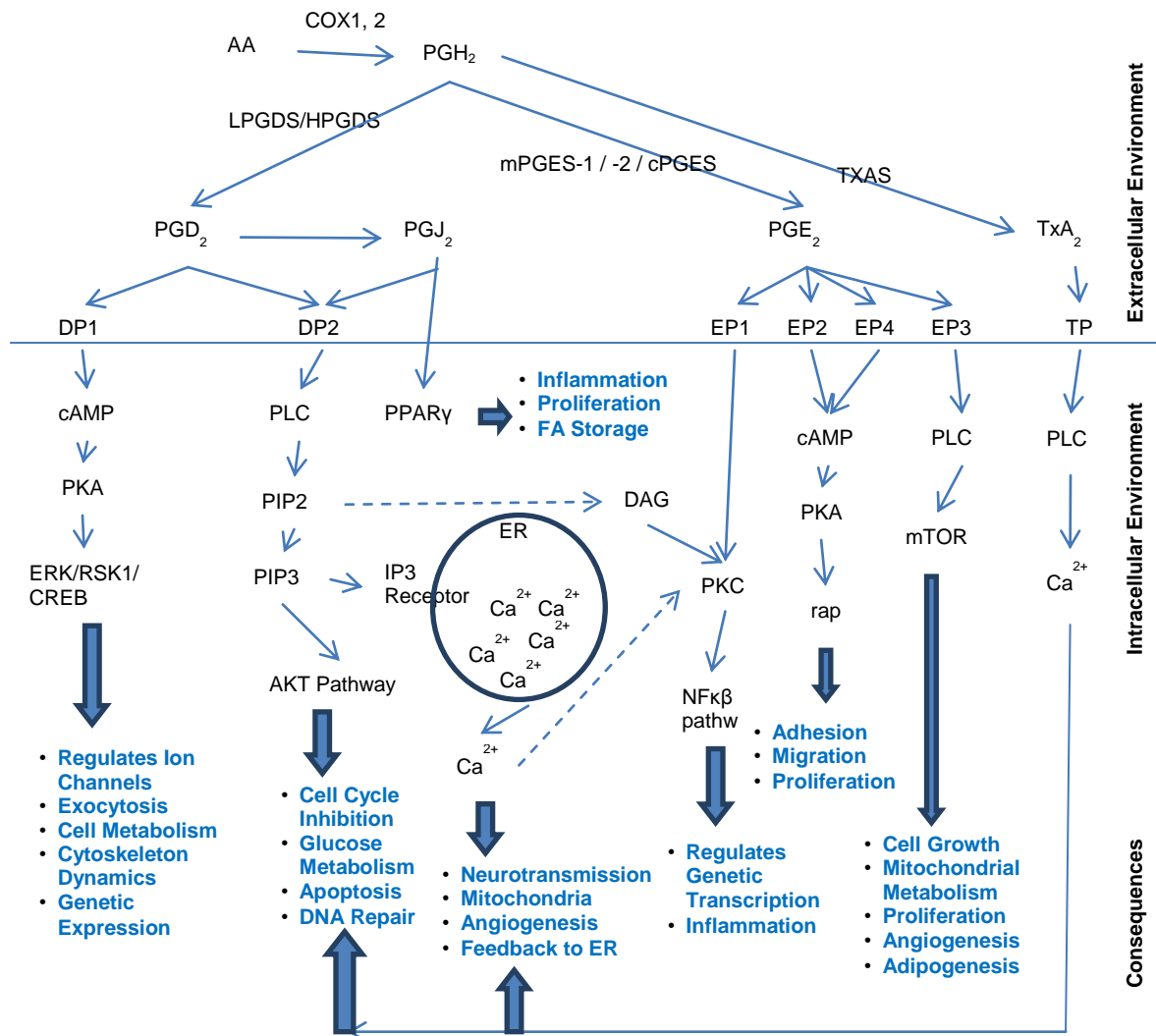


Figure 1.1. Summary of the biochemical pathways and their subsequent cellular effects influenced by PGD₂ and PGE₂.

2 OBJECTIVES

2.1 General Objective

Begin to define the general role of PGD₂ and its influence in glioblastomas, to contribute to a solid foundation of knowledge concerning one of the more prevalent prostaglandins in the brain.

2.2 Specific Objectives

- 1 Determine which enzymes and receptors related to PGD₂ are genetically expressed.
- 2 Determine which of these genes are translated in to proteins.
- 3 Determine if there is some expression of these proteins in the cell.
- 4 Determine if there is a relationship between the concentration and time of exposure of PGD₂ in the population size.
- 5 Observe the influence of exogenous PGD₂ in apoptosis and mitosis.
- 6 Determine if exogenous PGD₂ influences viability in gliomas.

3 MATERIALS AND METHODS

3.1 Cell Culture

Cell lines T-98G, U-251MG, A-172, U-138MG and U-87MG were analyzed. The cells were cultivated in Dulbecco's Modified Eagle Medium (DMEM) (*Life Technologies, NY, USA*) supplemented with 10% fetal bovine serum (FBS) (*Invitrogen, CA, USA*) and antibiotics (penicillin - 50 U/ml / streptomycin -50µg/ml) (*Invitrogen*). The flasks were maintained in incubators at 37 °C with an atmosphere of 5% CO₂ and 95% air until they reached an exponential phase of growth. The initial freezing of the cells was performed in medium supplemented with 20% serum and 10% dimethylsulfoxide (DMSO) at -80 °C. After 24 hours the cells were transferred to liquid nitrogen storage.

3.2 Growth Curves

The cells for the each of the cell lines were placed in 24-well plates containing four different cell concentrations: 1×10^4 /well, 3×10^4 /well, 5×10^4 /well, and 7×10^4 /well. The medium was changed every 24h. Counting the cells required first that the medium be removed and a phosphate buffer solution (PBS) containing 0.025% Trypsin / 0.02% EDTA be added to release the cells from the plate. The cells were then removed from the plate and store in 1.5 mL tubes. Then 10 µL was placed in a Neubauer Chamber for counting. The cells were counted after 24h, 48h, and 72 hours. The concentrations chosen to be used in treatments varied depending on the cell line. Refer to **Figures 3.1-3.5** below.

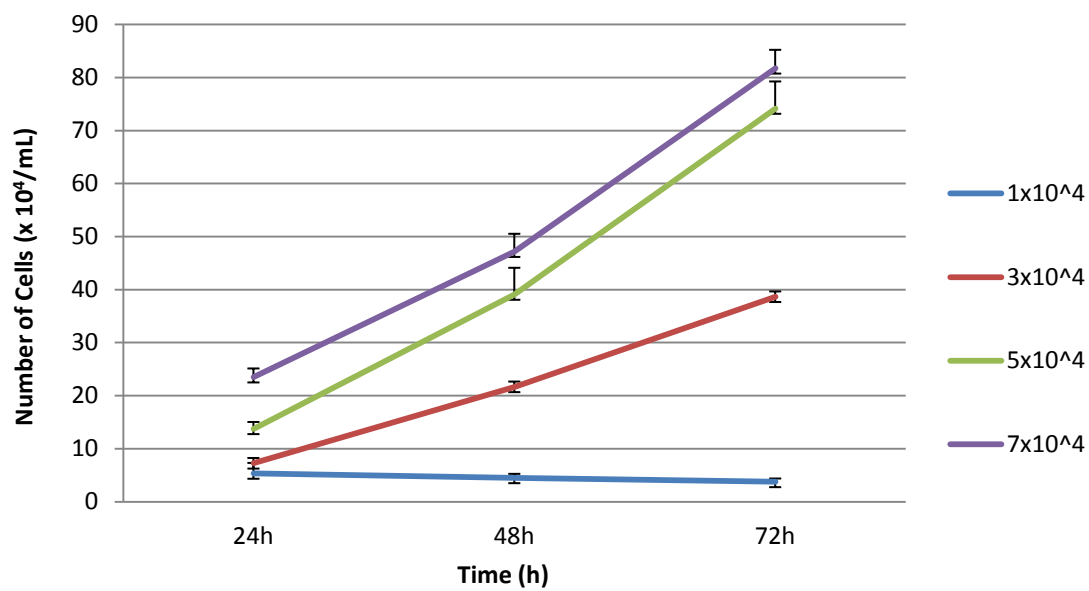
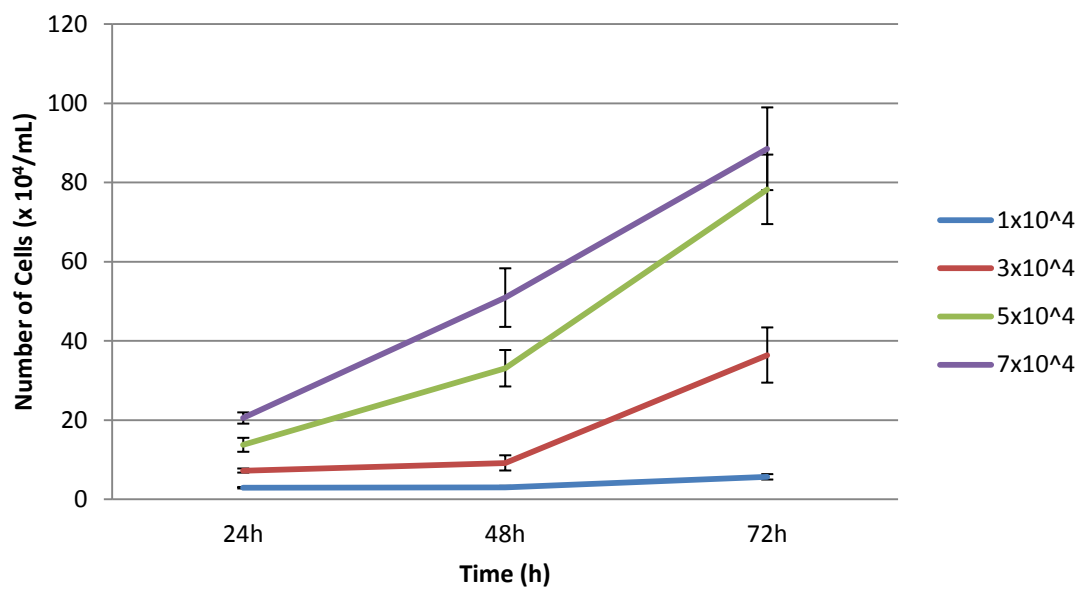
Figure 3.1 – Growth Curve- A-172**Figure 3.2 – Growth Curve- U-138MG**

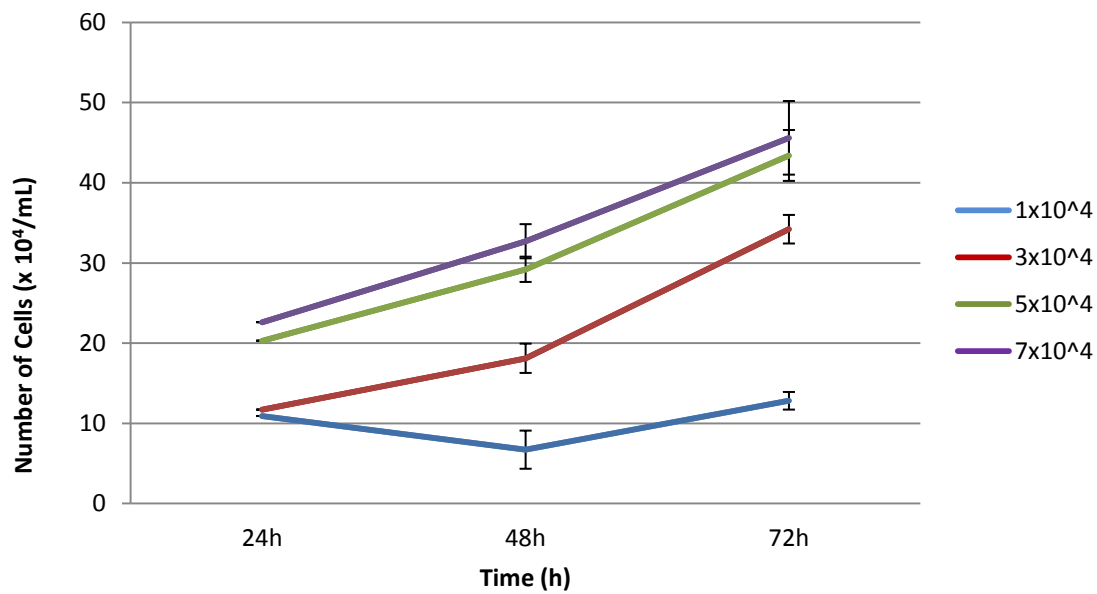
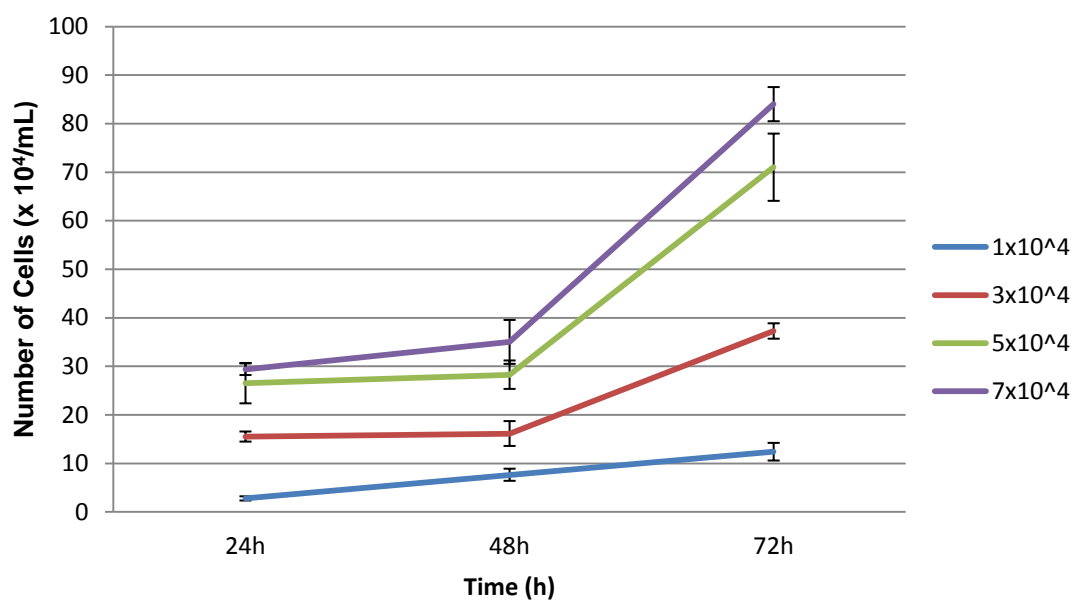
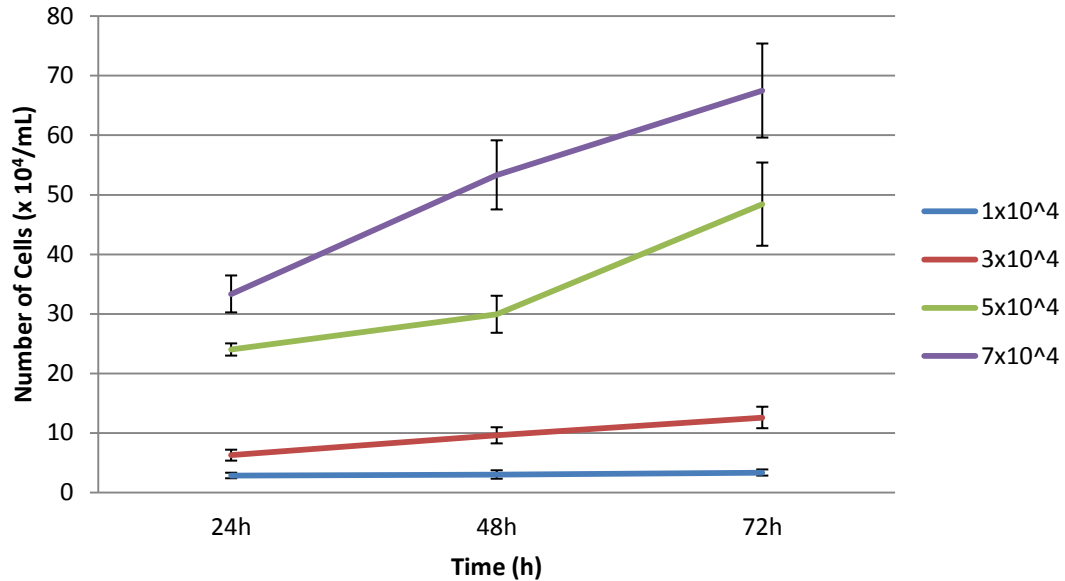
Figure 3.3 – Growth Curve- U-251MG**Figure 3.4** – Growth Curve- U-87MG

Figure 3.5 – Growth Curve- T-98G

3.3 Total RNA Extraction

For total RNA extraction, the five cell lines were each lysed with 1 mL of Trizol (Invitrogen) and left at room temperature for five minutes. After this period 0.2 mL of chloroform were added, and the samples were mixed for 15 seconds and left at room temperature for three minutes. Following this, the samples were centrifuged at 10,600 rpm (revolutions per minute) for 15 minutes at 4 °C. Next, the superior aqueous layer of the sample was removed and added to 0.5 mL of isopropanol to be centrifuged at 10,600 rpm for 10 minutes at 4 °C. The remaining precipitate was washed three times in 1 mL of 95% ethanol and centrifuged at 7,500 rpm for five minutes at 4 °C. Finally, the precipitate was resuspended in 20 μ L – 100 μ L of inactivated diethylpyrocarbonate (DEPC) treated water. The concentration of RNA was determined by a Multi-Volume Spectrophotometer System (BioTek, Winooski, VT, USA) reading the absorbancy at a ratio wavelength of A260 nm/A280 nm as the standard value; all the RNAs used in this study had presented between 1.8 and 2.0 purity. The purified RNA was stored and maintained in the -80 °C freezer.

3.4 Synthesis of complementary DNA

The basic methodology of RT-PCR extracted total RNA with Trizol, chloroform and isopropanol, and the purity of the RNA being between 1.8 and 2.0 was confirmed by a Multi-Volume Spectrophotometer System (*BioTek*). Complementary DNA was obtained by using Moloney Murine Leukemia Virus Reverse Transcriptase (M-MLV RT) (*Invitrogen*) in a reverse transcription polymerase chain reaction (RT-PCR) with approximately 1 µg of the RNA of interest. This reaction required, 1 µL of RNA inhibitor (RNase OUT), 2 µL of Random Primer, 2 µL of Dithiothreitol (DTT), 4 µL of RT buffer, 1 µL MMLV and approximately 1 µg of the RNA of interest. To amplify the cDNA, a thermocycler was used with the following predetermined temperatures and times: 21 °C for 10 min, 42 °C for 50 min, and 99 °C for 10 min. The amplification was confirmed by electrophoresis with a 1% agarose gel containing ethidium bromide revealed in a UV light capture system.

3.5 Primer Design

All primers used were designed from a base of sequences available in Genbank (www.ncbi.nlm.nih.gov) and complemented with the Primer 3 program (www.genome.wi.mit.edu/cgi-bin/primer/primer3_www.cgi). The specificity of each primer was verified through BLAST (<http://blast.ncbi.nlm.nih.gov/Blast.cgi>). The primers were synthesized by Invitrogen, Cayman Chemical, or Abcam. **TABLE 3.1** presents the primer sequences used.

3.6 Standardization of primers by RT-PCR

To determine the quality of the primers designed, each primer was analyzed at eight different temperatures (51 °C, 51.3 °C, 52.5 °C, 54.2 °C, 56.5 °C, 59.1 °C, 61.8 °C, 64.5 °C) using RT-PCR. The primers were designed for COX-1, COX-2, cPGES, mPGS-1, mPGS-2, H-PGDS, L-PGDS, EP1, EP2, EP3, EP4, DP-1, DP-2, and TP. These temperatures were tested to determine optimal temperature for primer annealing. Refer to **TABLE 3.1** for annealing temperatures and sizes of sequences.

TABLE 3.1. Primer sequences, annealing temperatures, and estimated band sizes by RT-PCR

<i>Primer</i>	<i>Sequence</i>	<i>Annealing Temp. (°C)</i>	<i>Band Size (base pairs)</i>
COX-1 sense	GCCTCAACCCCATAGTCCACCAA	59.1	275
COX-1 anti-sense	CAGACGACCCGCCTCATCCTCAT		
COX-2 sense	TGAAACCCACTCCAAACACA	61.8	187
COX-2 anti-sense	GAGAAGGCTTCCCAGCTTTT		
L-PGDS sense	CCAAACCGATAAGTGCATGAC	59.1	189
L-PGDS anti-sense	ACTTGCTTCCGGAGTTTATTGTG		
H-PGDS sense	ACCAGAGCCTAGCAATAGCA	56.5	261
H-PGDS anti sense	GCCCAAGTTACAGAGTTACCA		
PTGDR1 sense	GGGTA CTCTGTGCTCTACTC	56.5	270
PTGDR1 anti sense	CATAGTAAGCGCGATAAATTACGG		
PTGDR2 sense	CTTCTCAAACCTTGATGTGCC	56.5	103
PTGDR2 anti sense	TTGTTAAGTGCAGACTCTCAG		
mPGES1 sense	AAACATCACTCCCTCTCCCT	56.5	234
mPGES1 anti sense	GCCAGATTGTACCACTTACAC		
mPGES2 sense	GAAAGCTCGCAACAATAAATGAC	59.1	228
mPGES2 anti sense	CACTTCATCTCCTCCGTCCT		
cPGES sense	TTACATTAGTTGTCTCGGAGG	61.8	285
cPGES anti sense	CCCATGTTGTTTCATCATCTCAG		
EP2 sense	AGACGGACCACCTCATTCTC	56.5	207
EP2 anti sense	AACGCATTAGTCTCAGAACAGG		

TABLE 3.1 CONTINUED.

EP3 sense	CTTACCCTGCCAGTGTTCCT	56.5	181
EP3 anti sense	CGAGTACCTCCATTTCTTCTCTG		
EP4 sense	GACCTGTTGGGCACTTTGTT	56.5	274
EP4 anti-sense	TGGACGCATAGACTGCAAAG		
TP sense	GGCTGTCCTTCTGCTGAAC	56.5	348
TP anti-sense	GCTGAGGCGAGGCTGGAGAC		

3.7 Analysis of mRNA expression by RT-PCR

The cells were cultivated on 25 cm² plates and the total RNA was extracted using Trizol[®] (*Invitrogen*), according to the manufacturer's instructions. Synthesis of complementary DNA (cDNA) was done by RT-PCR using the MMLV-reverse transcriptase, following the manufacturer's instructions. The PCR was done using primers for the enzymes COX-1 and COX-2, cPGES, mPGS1, mPGS2, H-PGDS, L-PGDS, and the receptors EP1, EP2, EP3, EP4, DP-1, DP2, and TP. Amplification was confirmed by gel electrophoresis with 1% agarose containing ethyl bromide, and the product was viewed in a U.V. light capture system. The gene for the ribosomal subunit 18 was used as an endogenous control because of its constitutive expression.

3.8 Cell Line Selection

Firstly, the five available glioma cell lines were tested to verify which ones expressed messenger RNA for the PGD₂ and PGE₂ enzymes and receptors. The U-251MG and U-87MG cell lines were chosen because they expressed the mRNA necessary and they are compatible for *in vivo* studies using rats. The cell line A-172 was also chosen because it expressed the L-PGDS enzyme, challenging one of the only articles in the literature studying A-172 and PGD₂ production published by Payne et al. (2008).

3.9 HPLC-MS/MS

Samples were adjusted to 15% (v/v) with ice cold methanol and kept at 4 °C. Forty nanograms of freshly prepared internal standard (PGB₂-d₄) were added to each sample. After 15 minutes the sample was centrifuged (3000 rpm for 5 minutes), the precipitated proteins were removed, the supernatant was acidified to pH 3.0 with 0.1 M hydrochloric acid and immediately placed on C18 SPE cartridges preconditioned with 20 mL of 15% methanol, 20 mL water and 10 mL of hexane. Finally, eicosanoids were eluted in 15mL of methyl formate. The solvent was evaporated under nitrogen in the dark and the residue was dissolved in 100 µL of 70% (v/v) ethanol to be injected into the LC-MS/MS.

The Thermo Accela TSQ Quantum Max LC-MS/MS apparatus was operated in the electrospray negative ionization mode. Calibration lines were run for 21 prostanoids containing from 1 pg/µL to 200 pg/µL. Optimal conditions for each individual prostanoid were determined by direct infusion of a standard solution of 10 ng/µL. Typical parameters for use were: spray voltage 3500V; discharge current 80V; capillary temperature 350 °C; collision energy 13-30 V; tube lens 60-93 V; scan time 0.05-0.1 s.

A C18 Luna 2.0 x150 mm, 5 µm chromatography column from Phenomenex was used, and the sample volume was 5 µL at a flow rate of 350 µL/min with samples kept at 8 °C. Samples were run using Solvent A – H₂O (0.2% acetic acid); solvent C – acetonitrile (0.2% acetic acid). With a gradient as follows:- 0-10 min, 60% A : 40% C; 10.01-13 min, 60%-10% A : 40%-90% C; 13.01-15 min, 10% A : 90% C; 15-15.01 min, 10%-60% A : 90%-40% C; 15.01-19 min, 60% A : 40% C; 19.01 min-end, 100% A. The results were analyzed using Thermo XCalibur software.

3.10 Dosage Response Curve

To confirm that PGE₂ and PGD₂ affect the growth of GBM, each prostaglandin was added to the three cell lines at varying concentrations (0.03µM; 0.17 µM; 0.35 µM; 0.88 µM; 1 µM; 5 µM; 10 µM). The concentrations less than 1 µM evaluated responses closer to physiological

conditions. The concentrations from 1 μM to 10 μM tested supraphysiological conditions. Based on the standardized growth curves, the ideal number of cells in each cell line was chosen, cultivated and treated in a 24-well plate.

Twelve hours after plating the cells in three 24-well plates, the medium was changed with medium containing PGE_2 or PGD_2 at different concentrations. The experimental controls included one treatment with normal medium containing DMEM/FBS and one treatment of medium containing DMEM/FBS with DMSO or Ethanol; the carriers in which the stocks of PGD_2 and PGE_2 were diluted. Each treatment was applied to at least three samples in each plate every 24 hours. The cells were collected and counted in a Neubauer Chamber at time intervals of 24 hours, 48 hours, and 72 hours. All treatments were tested three times with an $n=3$.

3.11 Immunohistochemical Reactions

In order to confirm the presence of the enzymes and receptors in the cell lines of interest, cells were cultivated and fixed in 4% formaldehyde in 0.1 M phosphate buffer and later washed three times in PBS. Blocking the endogenous peroxidase was done with 2% of H_2O_2 in methanol/ H_2O (1:1) for 30 minutes followed by various washes (three times with distilled water and three times with PBS). Blocking the nonspecific binding sites was done with a 2% Normal Donkey Serum/Bovine Serum Albumin solution in 0.2% PBS – Triton X-100 (PBST) for one hour. The samples were then incubated overnight with their respective antibodies at concentrations varying between 1:50 – 1:200, diluted in PBST at room temperature. The negative experimental controls received only PBS-T. After this time, the samples were washed three times using PBST, then the secondary biotinylated antibodies (1:100) were added for 1.5 hours. After washing again with PBST three times, Streptavidin-Horseradish Peroxidase (1:100) was added for one hour. The samples were washed again with PBST three times and then washed one time with PBS. 3,3'-Diaminobenzidine (DAB)/ H_2O_2 was added and the reaction was observed and then stopped using distilled water. The samples were then prepared for analysis using mounting medium and glass cover slips. Primary and secondary antibodies were obtained from the

Cayman Chemical Company, Ann Arbor, MI, USA, and the Streptavidin-Horseradish Peroxidase was from General Electric, Rio de Janeiro, RJ, Brazil.

3.12 Viability Test

To confirm the viability of cells exposed to treatments of PGD₂ the MTT assay was chosen because it is a yellow tetrazolium salt converted to a purple formazan product by active mitochondrial dehydrogenases. The cells were cultivated on 96-well plates and treated with PGD₂. After 20 hours from the first treatment of PGD₂, 10 µL of MTT were applied to the cells and incubated for another four hours at 37 °C. At the end of this time, or rather 24 hours after the first PGD₂ treatment, 100 µL of 0.04 M HCl in isopropanol was added for five minutes to dissolve the formazan product. The plate was then inserted in a Multi-Volume Spectrophotometer System (*BioTek*) and the absorbance was read at a wave-length of 595 nm. All experiments had an n=3.

3.13 Apoptosis and Mitosis Test

Apoptosis and mitosis were observed in the cells by first cultivating the three cell lines on glass disks placed in 24-well plates. They were treated every 24 hours for a total of 72 hours then collected and fixed with 4% formaldehyde in 0.1M phosphate buffer. The samples were then washed three times with PBS 1X then a Hoechst 33342 stain (50µL Hoechst/ 10mL PBS) was applied and placed in a dark environment for 10 minutes. The glass disks containing the stained cells were then removed and secured on glass slides using mounting medium, Vectashield (*Vector Laboratories*, Burlingame, CA, USA), for observation and analysis. Ten randomly selected areas were photographed of each glass disk and the number of cells in apoptosis and the number of cells in mitosis were counted separately. All experiments had an n=4.

3.14 Data Analysis

Dose response tests and viability tests are presented as the mean \pm SEM. Using the *GraphPad Prism 5* software the significance was determined by a two-way ANOVA post-test with Bonferroni test. The significance of the apoptosis and mitosis experiments was verified through a parametric unpaired Student's T-test. The differences were considered significant with $p < 0.05$ and highly significant with $p < 0.001$. The significance of the p-value is represented in the figures by "*" ($* < 0.05$, $** < 0.001$, $*** < 0.0001$).

4 RESULTS

4.1 PCR

The primers designed to amplify the segments of the DNA coding for the enzymes and receptors in PGD₂ and PGE₂ production pathway showed varying results. First, COX-1 and COX-2 were found to be expressed in all five cell lines. The gene for L-PGDS was also found in all five cell lines. H-PGDS expression was extremely weak. The DP1 receptor was expressed in the U-251MG, U-138MG and U-87MG cell lines. The DP2 receptor demonstrated a weak expression in all cell lines. The TP receptor was expression in all five cell lines. PGE₂ receptors EP2 and EP3 were expressed in all five cell lines. Cytosolic PGES was also expressed in the U-183MG, U-87MG and T-98G cell lines. **TABLE 4.1** shows gene amplification through RT-PCR in all five cell lines. **TABLE 4.2** summarizes the RT-PCR results in the cell lines studied.

TABLE 4.1 RT-PCR for genes involved in the PGE₂ and PGD₂ pathways in cell lines A-172, U-138MG, U-251MG, U-87MG, T-98G

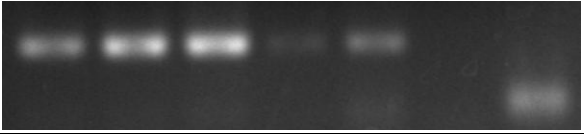
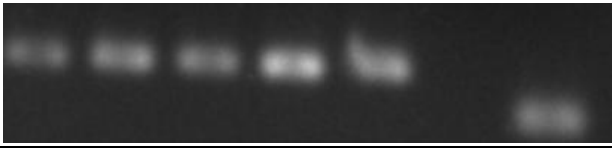
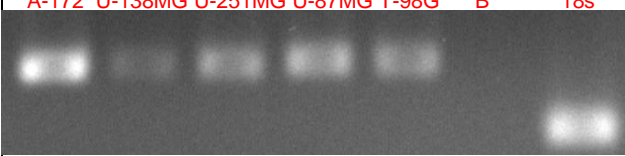
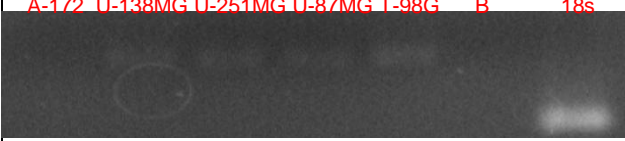
COX-1	A-172 U-138MG U-251MG U-87MG T-98G B 18s 	275 bp
COX-2	A-172 U-138MG U-251MG U-87MG T-98G B 18s 	187 bp
L-PGDS	A-172 U-138MG U-251MG U-87MG T-98G B 18s 	189 bp
H-PGDS	A-172 U-138MG U-251MG U-87MG T-98G B 18s 	261 bp
DP1	A-172 U-138MG U-251MG U-87MG T-98G B 18s 	270 bp
DP1	U-251MG U-87MG B 18s 	270 bp

TABLE 4.1 Continued

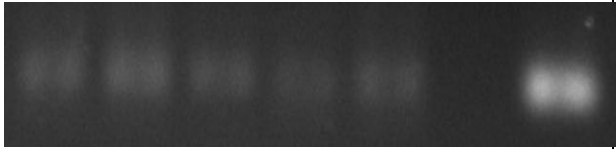
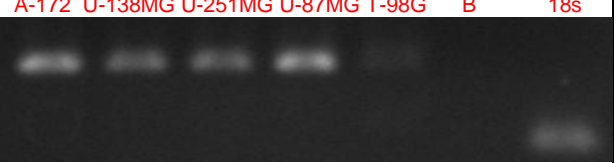
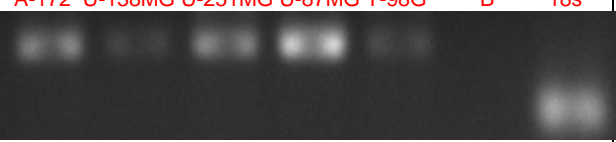
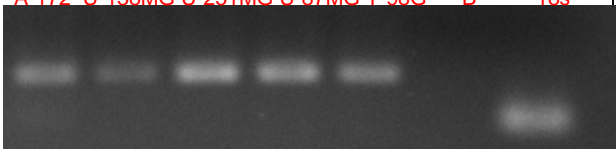
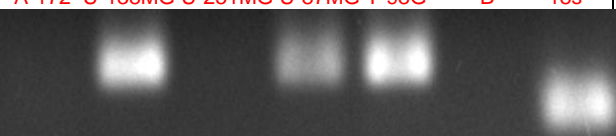
DP2	A-172 U-138MG U-251MG U-87MG T-98G B 18s 	103 bp
TP	A-172 U-138MG U-251MG U-87MG T-98G B 18s 	348 bp
EP2	A-172 U-138MG U-251MG U-87MG T-98G B 18s 	207 bp
EP3	A-172 U-138MG U-251MG U-87MG T-98G B 18s 	181 bp
cPGES	A-172 U-138MG U-251MG U-87MG T-98G B 18s 	285 bp

TABLE 4.2. Summary of mRNA expression in cell lines A-172, U-138MG, U-251MG, U-87MG, T-98G.

Primer	A-172	U-138MG	U-251MG	U-87MG	T-98G
<i>COX-1</i>	√	√	√	√	√
<i>COX-2</i>	√	√	√	√	√
<i>L-PGDS</i>	√	√	√	√	√
<i>H-PGDS</i>	-	√	√	√	√
<i>mPGES-2</i>	√	√	√	√	√
<i>cPGES</i>	-	√	-	√	√
<i>DP1</i>	-	√	√	√	-
<i>DP2</i>	√	√	√	√	√
<i>TP</i>	√	√	√	√	√
<i>EP1</i>	-	-	-	-	-
<i>EP2</i>	√	√	√	√	√
<i>EP3</i>	√	√	√	√	√
<i>EP4</i>	√	√	√	√	√

4.2 Immunohistochemistry

To confirm the translation of genes expressed in the PCR to proteins present in the cell cytoplasm and membrane immunohistochemistry was successfully performed in the U-251MG, U-87MG, and A-172 cell lines. **Figure 4.1** represents the results observed using the cell line U-87MG. Although the RT-PCR for the DP1 and DP2 genes appeared to be weak, there was a clear presence of both receptors in all three cell lines. L-PGDS and TP are also found in all three cell lines. Other antibodies revealed the presence of all three PGE₂ enzymes as well as the EP2 and EP4 receptors in two cell lines. **TABLE 4.3** summarizes the immunohistochemical results.

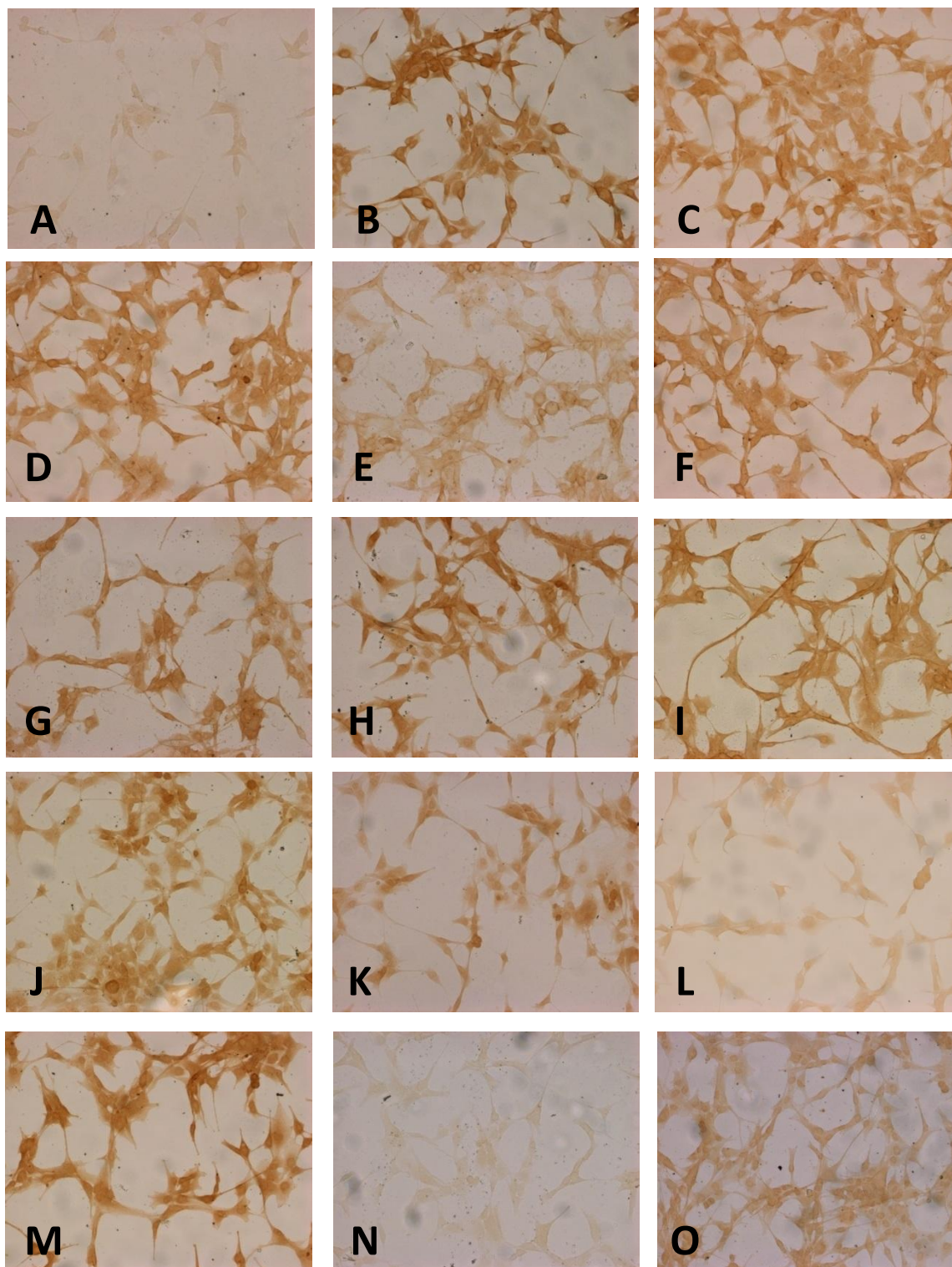


Figure 4.1 Immunohistochemistry results of U-87MG. Images show a general cytoplasmic and membrane staining. Image: (A) Anti-Rabbit control for images (B - K), (B) COX-2, (C) cPGES, (D) EP2 receptor, (E) EP4 receptor, (F) mPGES1, (G) DP1 receptor, (H) DP2 receptor, (I) mPGES2, (J) Thromboxane synthase (TXAS), (K) TP receptor, (L) Anti-mouse control for COX-1, (M) COX-1, (N) Anti-rat control for L-PGDS, and (O) L-PGDS.

4.3 HP-LC/MS/MS

The presence of PGD₂ and PGE₂ was confirmed by HP-LC/MS/MS in two cell lines. Although PGE₂ maintains the strongest presence, PGD₂ also has a detectable level of synthesis. **Figure 4.2** shows production in the U-251MG cell line. **Figure 4.3** shows the production in the U-87MG cell line. The A-172 cell line did not possess enough PGD₂ to be detected.

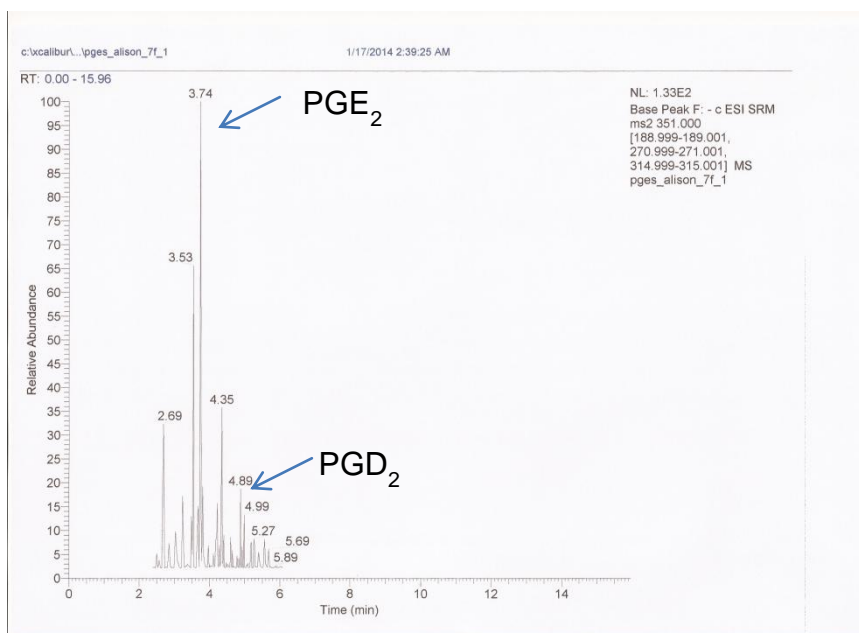


Figure 4.2 The relative abundance of PGE₂ and PGD₂ measured in cell line U-251MG. PGD₂ is present at around one-fifth of the amount of PGE₂ detected.

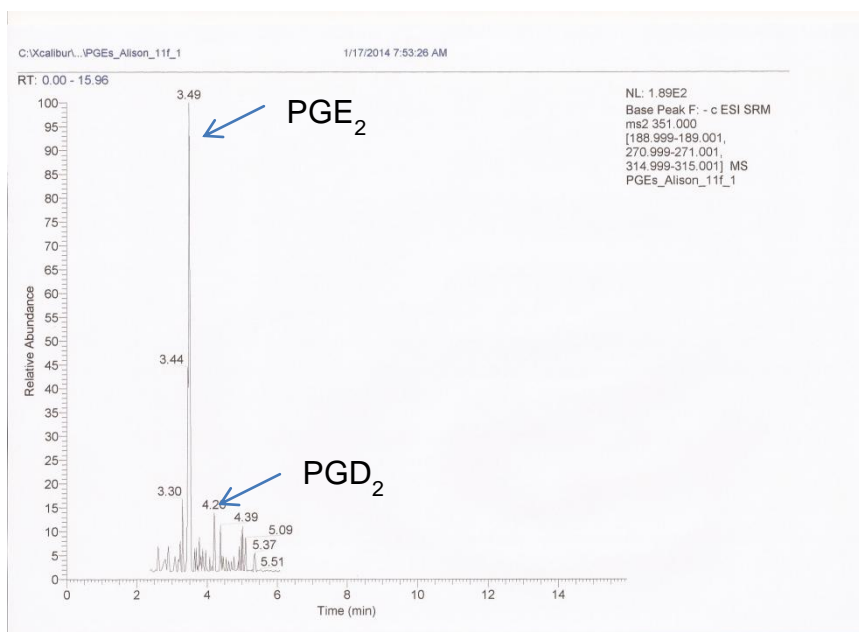


Figure 4.3 The relative abundance of PGE₂ and PGD₂ measured in cell line U-87MG. PGD₂ is present at around one-sixth of the amount of PGE₂ detected.

4.4 Dose-Response Curves

Investigating the general cellular response to varying concentrations of PGD₂ treatments was divided into two parts. The first part investigated the cellular response to concentrations of PGD₂ closer to potential physiological conditions, and the second part investigated supraphysiological concentrations. In the first part, cell lines U-251MG and A-172 demonstrated a significant increase in cell count over time and concentration. This matched the responses seen when treated with PGE₂. The 0.35 μM PGD₂ concentration proved to be more influential in cell count for both cell lines. In the supraphysiological treatments, cell lines U-251MG, A-172 and U-87MG all responded with a significant decrease in cell count. Over 72h, the cell counts decreased the most in response to the 10μM PGD₂ treatment. **Figures 4.4** and **4.6** represent treatments made with PGD₂ concentrations close to physiological conditions. **Figures 4.5** and **4.7** reflect the same concentrations applied with PGE₂. **Figures 4.8 – 4.10** represent treatments of PGD₂ applied with supraphysiological concentrations. Results were considered significant when $p < 0.05$.

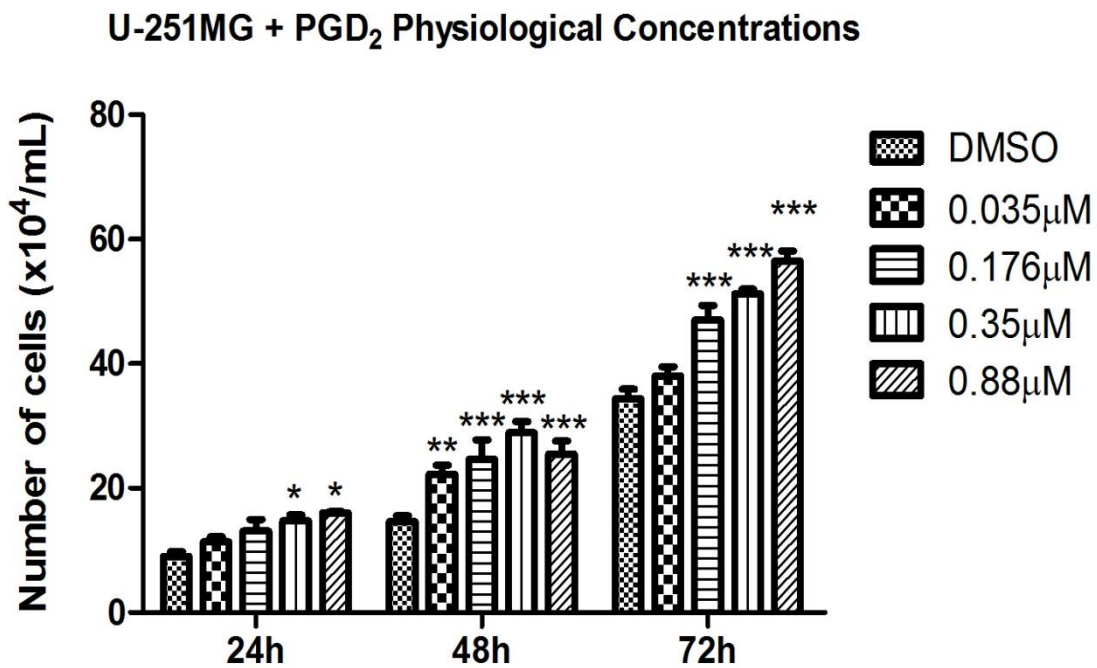


Figure 4.4 Cell counts of samples treated with PGD₂ concentrations close to physiologically encountered PGD₂ levels over the span of 72h in cell line U-251MG. The difference between the Control (DMSO) and the treatment was considered significant with $p < 0.05$ and highly significant with $p < 0.001$. The significance of the p-value is represented in the figures by “*” ($* < 0.05$, $** < 0.001$, $*** < 0.0001$). (n=4).

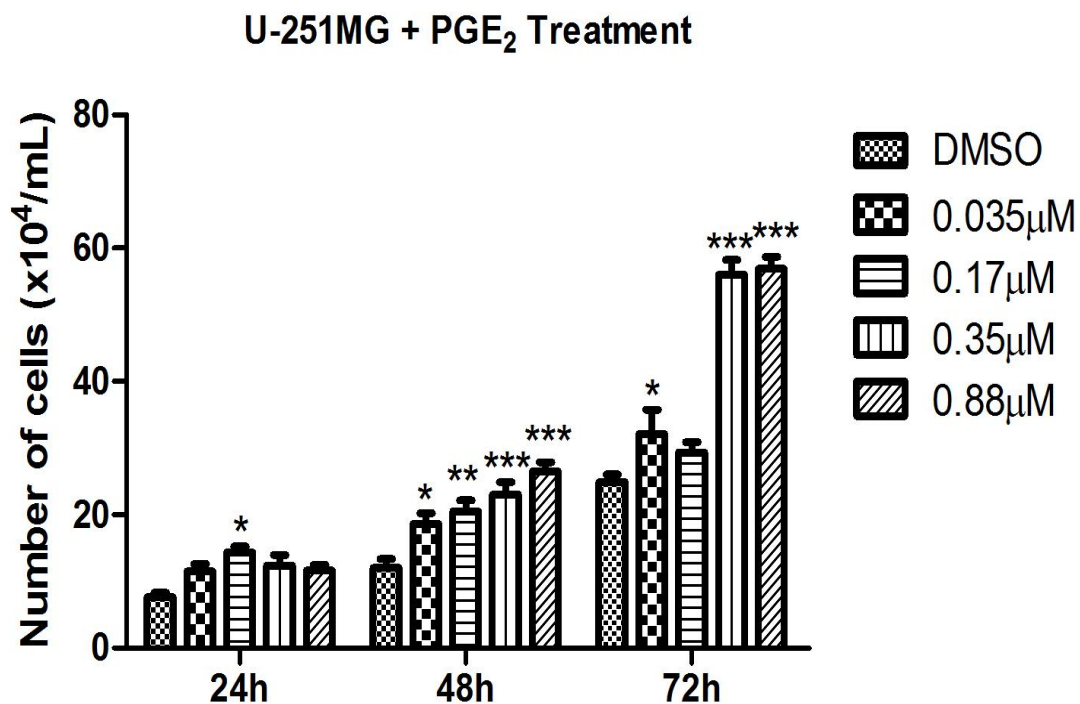


Figure 4.5 Cell counts of samples treated with PGE₂ concentrations reflecting the PGD₂ treatments over the span of 72h in cell line U-251MG. The difference between the Control (DMSO) and the treatment was considered significant with $p < 0.05$ and highly significant with $p < 0.001$. The significance of the p-value is represented in the figures by "*" ($* < 0.05$, $** < 0.001$, $*** < 0.0001$). (n=4).

A-172 + PGD₂ Physiological Concentrations

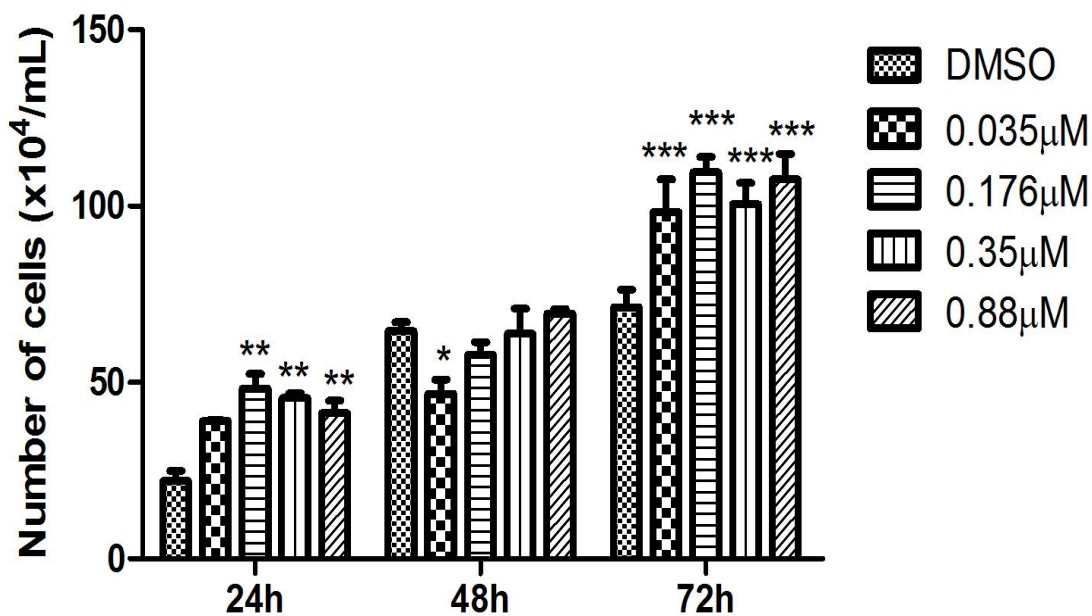


Figure 4.6 Cell counts of samples treated with PGD₂ concentrations close to physiologically encountered PGD₂ levels over the span of 72h in cell line A-172. The difference between the Control (DMSO) and the treatment was considered significant with $p < 0.05$ and highly significant with $p < 0.001$. The significance of the p-value is represented in the figures by "*" ($* < 0.05$, $** < 0.001$, $*** < 0.0001$). (n=3).

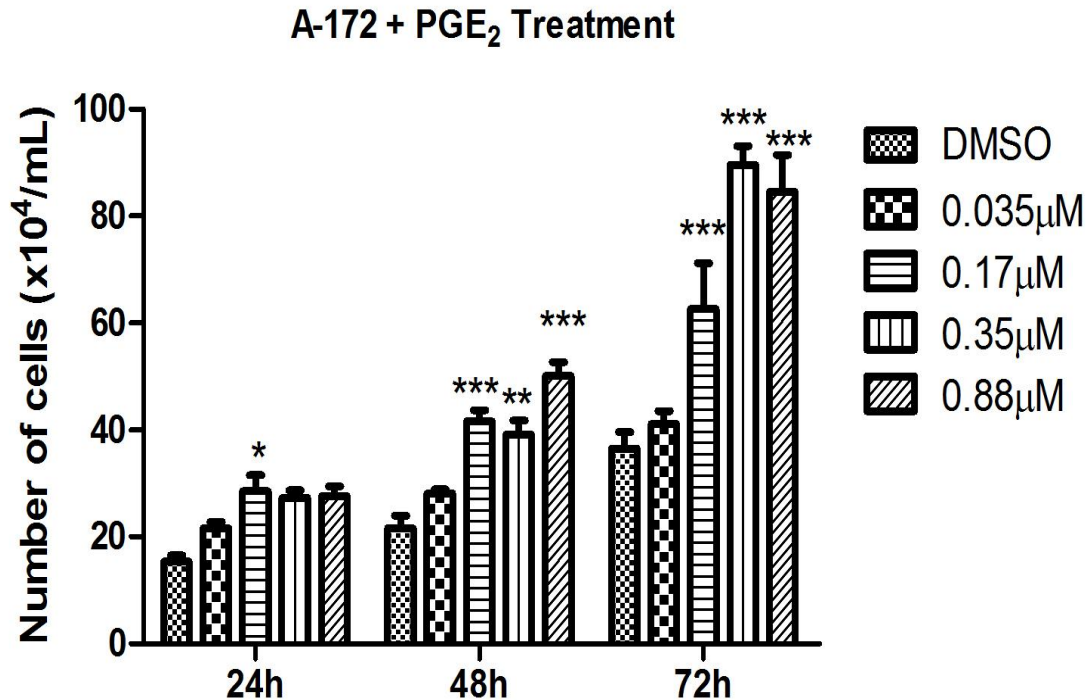


Figure 4.7 Cell counts of samples treated with PGE₂ concentrations reflecting the PGD₂ treatments over the span of 72h in cell line A-172. The difference between the Control (DMSO) and the treatment was considered significant with $p < 0.05$ and highly significant with $p < 0.001$. The significance of the p-value is represented in the figures by “*” ($* < 0.05$, $** < 0.001$, $*** < 0.0001$). (n=3).

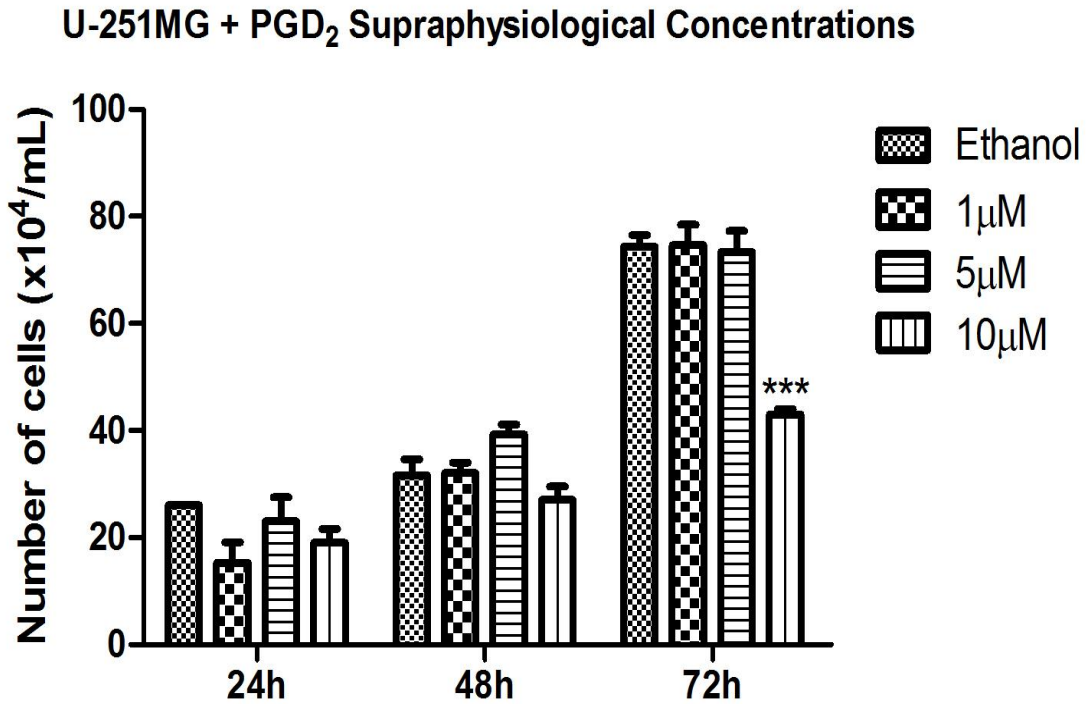


Figure 4.8 Cell counts of samples treated with PGD₂ concentrations above physiologically encountered levels over the span of 72h in cell line U-251MG. There was a significant decrease at 72h with the 10 μM treatment. The difference between the Control (Ethanol) and the treatment was considered significant with $p < 0.05$ and highly significant with $p < 0.001$. The significance of the p -value is represented in the figures by “*” ($* < 0.05$, $** < 0.001$, $*** < 0.0001$). (n=3).

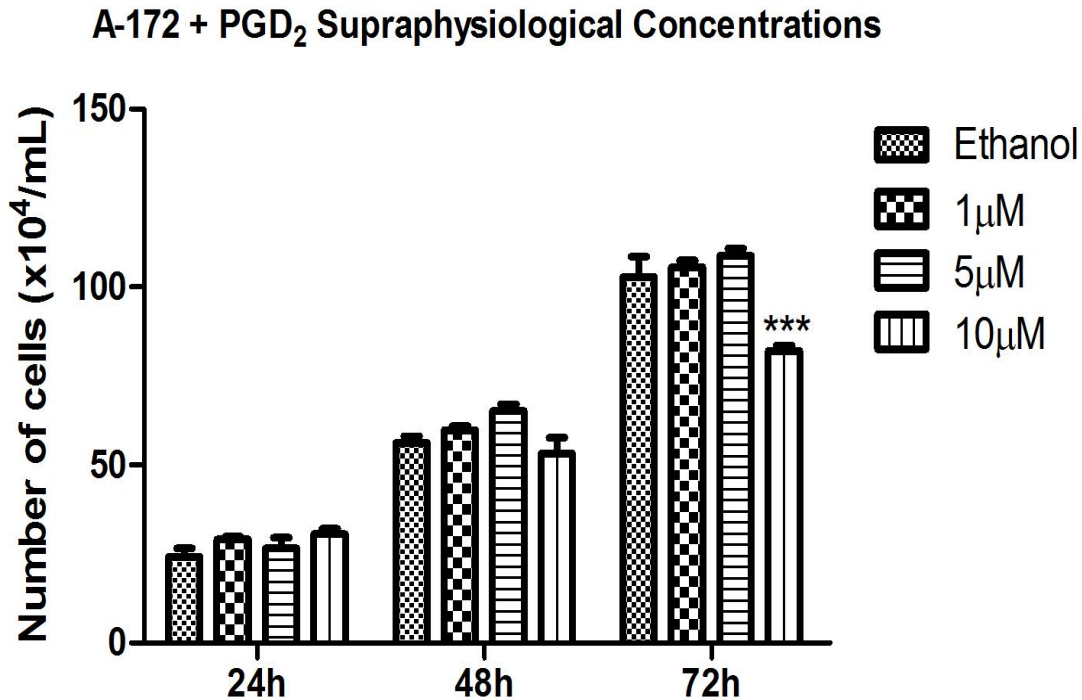


Figure 4.9 Cell counts of samples treated with PGD₂ concentrations above physiologically encountered levels over the span of 72h in cell line A-172. There was a significant decrease at 72h with the 10 µM treatment. The difference between the Control (Ethanol) and the treatment was considered significant with $p < 0.05$ and highly significant with $p < 0.001$. The significance of the p-value is represented in the figures by “*” ($* < 0.05$, $** < 0.001$, $*** < 0.0001$). (n=2).

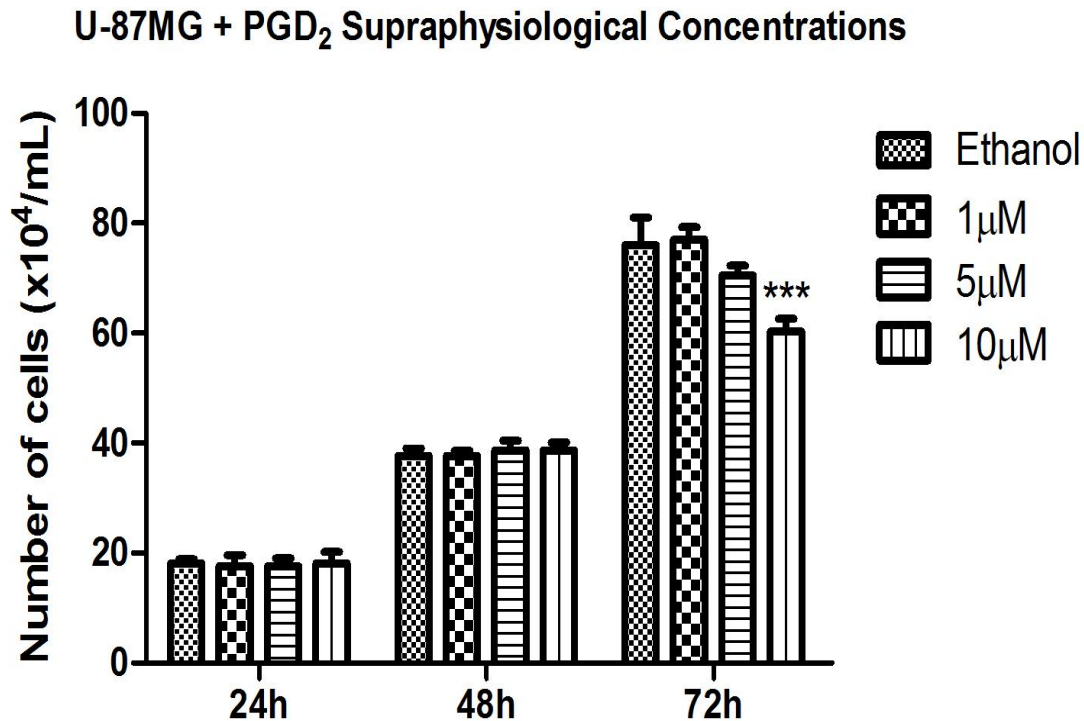


Figure 4.10 Cell counts of samples treated with PGD₂ concentrations above physiologically encountered levels over the span of 72h in cell line U-87MG. There was a significant decrease at 72h with the 10 µM treatment. The difference between the Control (Ethanol) and the treatment was considered significant with $p < 0.05$ and highly significant with $p < 0.001$. The significance of the p-value is represented in the figures by “*” ($* < 0.05$, $** < 0.001$, $*** < 0.0001$). (n=2).

4.5 Viability Tests (MTT)

Figures 4.11, 4.12 and-4.13 show the viability of cells treated for 72 hours with nanomolar (0.35 μM) and micromolar concentrations of PGD_2 in three cell lines. The treatment with 10 μM PGD_2 produced a significantly negative response in all three cell lines, causing their viability to decrease as time progressed. At 72 hours a very significant difference was observed.

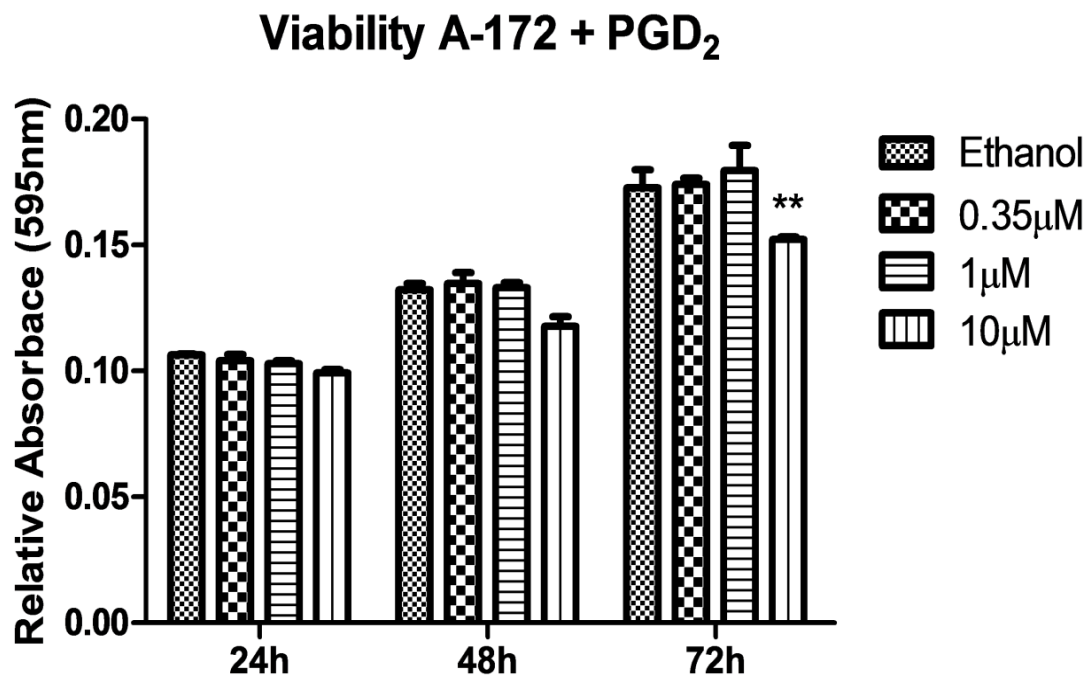


Figure 4.11 The viability of A-172 cells treated during a 72 hour period with 0.35 μ M, 1 μ M and 10 μ M of PGD₂. There was a significant decrease at 72h with the 10 μ M treatment. The difference between the Control (Ethanol) and the treatment was considered significant with $p < 0.05$ and highly significant with $p < 0.001$. The significance of the p-value is represented in the figures by “*” ($* < 0.05$, $** < 0.001$, $*** < 0.0001$). (n=2).

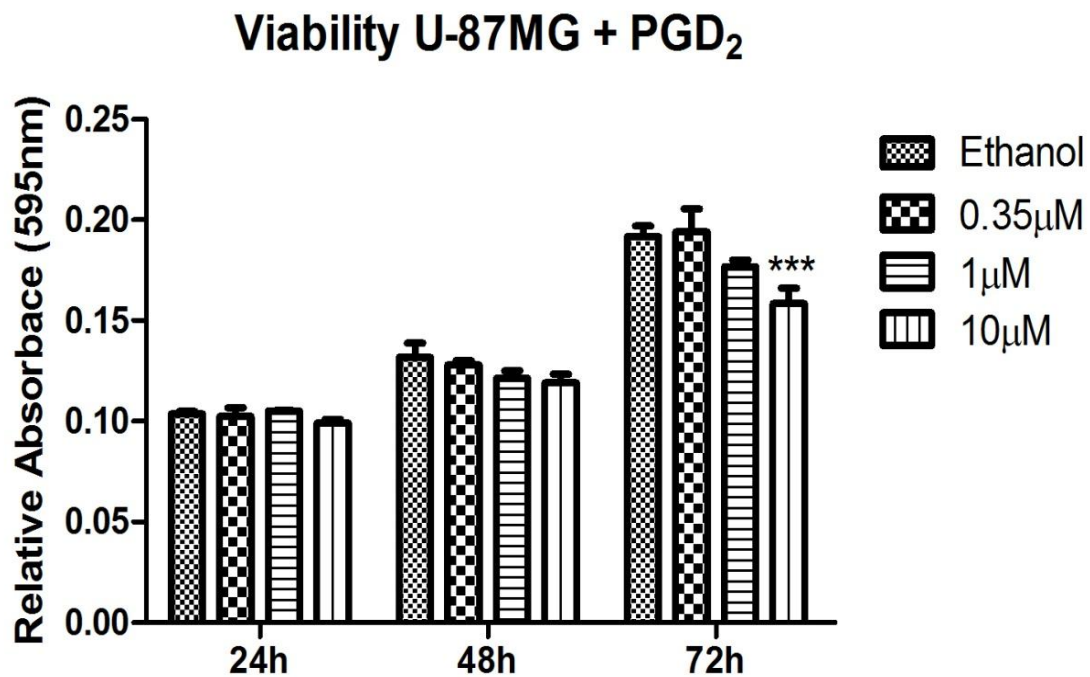


Figure 4.12 The viability of U-87MG cells treated during a 72 hour period with 0.35 µM, 1 µM and 10 µM of PGD₂. There was a significant decrease at 72h with the 10 µM treatment. The difference between the Control (Ethanol) and the treatment was considered significant with $p < 0.05$ and highly significant with $p < 0.001$. The significance of the p-value is represented in the figures by “*” ($* < 0.05$, $** < 0.001$, $*** < 0.0001$). (n=2)

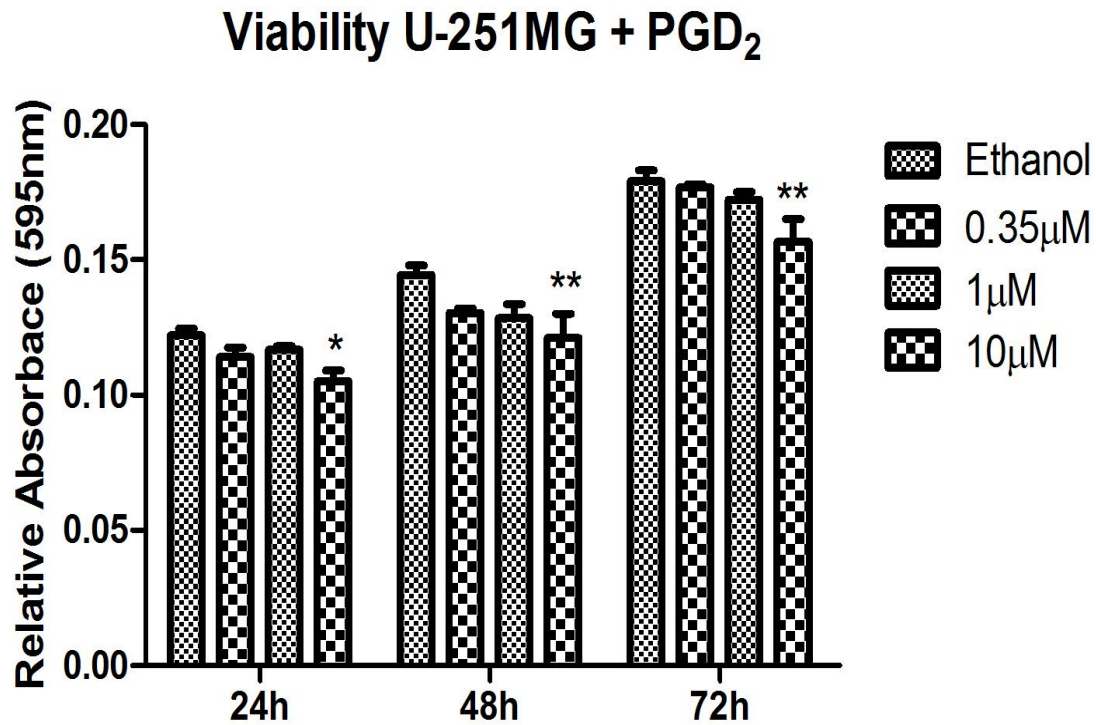


Figure 4.13 The viability of U-251MG cells treated during a 72 hour period with 0.35 µM, 1 µM and 10 µM of PGD₂. There was a significant decrease at 24h, 48h and 72h with the 10 µM treatment. The difference between the Control (Ethanol) and the treatment was considered significant with $p < 0.05$ and highly significant with $p < 0.001$. The significance of the p-value is represented in the figures by “*” ($* < 0.05$, $** < 0.001$, $*** < 0.0001$). (n=2)

4.6 Apoptotic and Mitotic Responses

In the search for the influence of PGD₂ on cellular activities such as apoptosis and mitosis, it was observed that PGD₂ applied in a 10 μM concentration for 72 hours created no significant change in apoptotic events in the cell lines when compared to the ethanol control. However, this 10 μM PGD₂ treatment did express a decreasing tendency in U-251MG where $p= 0.35$. **Figure 4.14** represents the apoptotic response of three cell lines to PGD₂ treatment.

In addition to this, the same application of PGD₂ demonstrated a significant decrease in the mitotic activity in cell line U-251MG. Also, no significant change was observed in A-172 and U-87MG. **Figure 4.15** represents the mitotic responses to PGD₂ treatment in three cell lines. **TABLE 4.4** shows representative images of the Hoechst staining in three cell lines. Note: There is also an observable decrease in cell count in the images of PGD₂ treated cells.

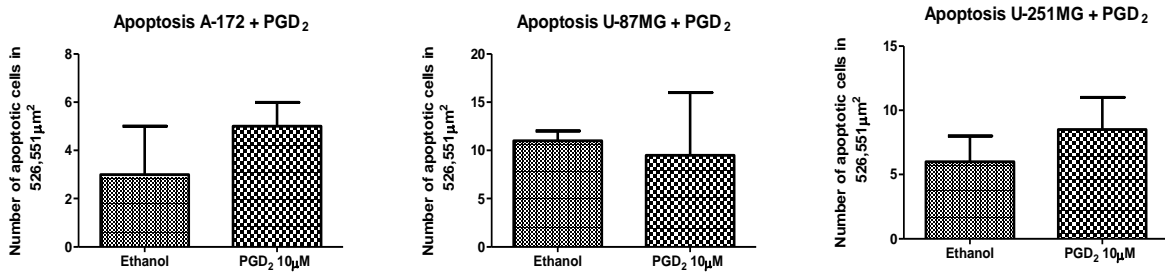


Figure 4.14 The Hoechst staining revealed an insignificant difference in apoptotic activity caused by 10 μM PGD₂ treatments over a 72h period in all three cell lines. The difference between the Control (Ethanol) and the treatment was considered significant with $p < 0.05$. (n=2, performed in quadruplicates)

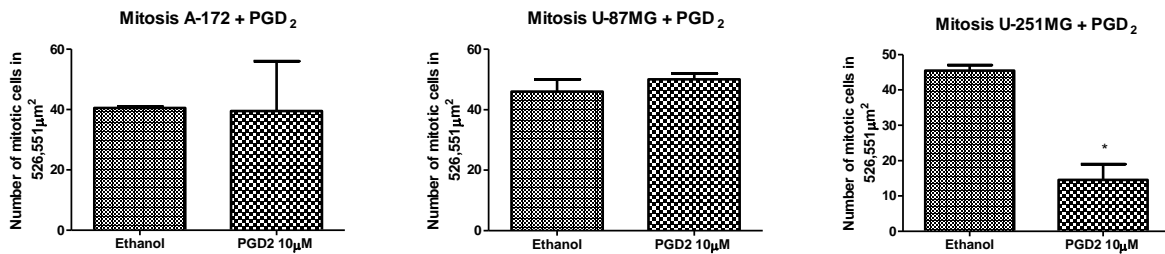
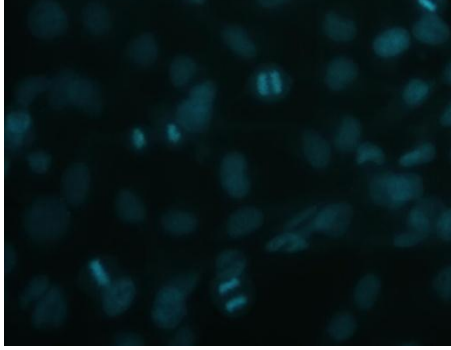
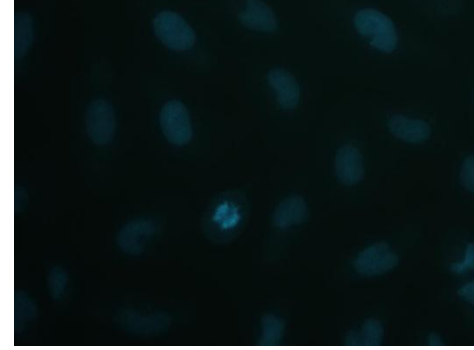
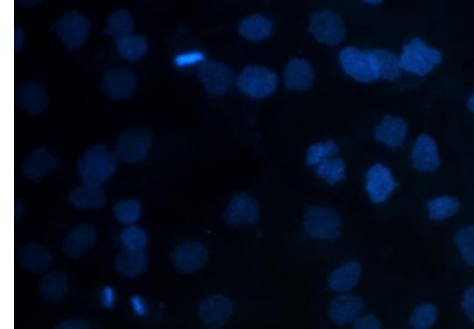
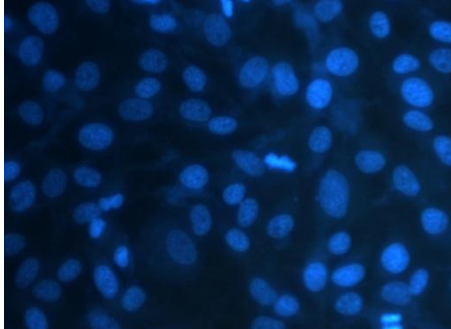


Figure 4.15 The Hoechst staining revealed a significant difference in mitotic activity caused by 10 μM PGD₂ treatments over a 72h period in the A-172 and U-251MG cell lines. The difference between the Control (Ethanol) and the treatment was considered significant with $p < 0.05$. The significance of the p-value is represented in the figures by “*” ($* < 0.05$, $** < 0.001$, $*** < 0.0001$). (n=2, performed in quadruplicates).

TABLE 4.4 PGD₂ treated cells and their respective controls with Hoechst staining in UV light.

Cell Line	Control- Ethanol	Treated- 10μM PGD ₂
U-251MG		
A-172		
U-87MG		

5 DISCUSSION

Glioblastoma cells have developed mechanisms that aid their survival against modern forms of chemotherapy, radiation therapy, and surgery. Endeavoring to obtain a deeper understanding of the biochemical pathways utilized by GBM cells, we investigated PGD₂'s influence on GBM. PGD₂ treatments have already demonstrated anti-tumorigenic effects in human colon cancer and in lung carcinoma (Murata et al., 2011; Yoshida et al., 1998). Two main questions were presented to address PGD₂'s relationship with GBM; is PGD₂ produced in GBM, and does PGD₂ influence critical cellular activities in GBM?

5.1 The Confirmed Presence of the PGD₂ Synthesis Pathway

To address the first question regarding GBM's ability to produce PGD₂, we firstly performed RT-PCR tests, then immunohistochemical tests, and finally HPLC tandem mass spectrometry. First, we needed to examine if the genes of all of the necessary enzymes and receptors related to PGD₂ in the five cell lines were present. For this we performed RT-PCRs (see **Table 4.1**). We began with COX-1 and COX-2, the two main enzymes that convert AA into PGG₂ and subsequently into PGH₂. COX-1 and COX-2 were expressed in all five cell lines which can be confirmed by other studies previously published by our lab and by the Human Protein Atlas (HPA) (Gomes and Colquhoun, 2012; Uhlen et al., 2012). We then produced an immunohistochemical staining using HRP/DAB and confirmed COX-1 and COX-2 presence in the cytoplasm of the A-172, U-87MG, and U-251MG cell lines. The HPA found little COX-1 RNA expression in U-138MG and U-87MG, and no RNA expression was seen in U-251MG, which is not what was observed in our study. However, they did record RNA expression and strong protein antibody staining of COX-2 in U-138MG, U-251MG, and U-87MG, confirming what was observed in our study. Refer to **Table 5.1** for a summary of The Human Protein Atlas' findings in GBM cell lines.

The next component necessary for the production of PGD₂ is the conversion of PGH₂ by the enzymes H-PGDS or L-PGDS. The RT-PCR tests demonstrated that the gene for H-PGDS was not

expressed in A-172, but appears to have a faint expression in the other four cell lines. There are no other studies to confirm H-PGDS expression in these cell lines, and there was no antibody available to purchase for performing an immunohistochemical test. Also, The Human Protein Atlas found no expression of H-PGDS in GBM in both *in vitro* and *in vivo* (Uhlen et al., 2012). The gene for L-PGDS was expressed in all five cell lines, with a more obvious expression in the A-172 cell line. In Payne's study, L-PGDS was not expressed in A-172 during their investigation of the transition of low-grade astrocytomas to GBM, presenting potentially conflicting data (Payne et al., 2008). The HPA indicated that L-PGDS has some RNA expression in the cell line U-87MG, and no expression in U-138MG and U-251MG. Our RT-PCR presented observable RNA expression of L-PGDS in five cell lines. The protein antibody staining performed by the HPA of GBM samples removed from patients showed a strong presence of L-PGDS (Uhlen et al., 2012). Our immunohistochemistry performed on the immortalized cell lines A-172, U-251MG, and U-87MG also demonstrated the observable presence of L-PGDS in the cytoplasm. The HPA has not yet performed any immunohistochemistry for L-PGDS in these same cell lines. According to our HPLC tandem mass spectrometry, the relatively low abundance of PGD₂ could be explained by the presence of only one of the two PGD₂ synthases.

A possible explanation to the seemingly conflicting data between our results combined with the HPA results and those observed by Payne's study, is that once the transition of a low-grade glioma becoming a GBM is complete, the cells begin to produce L-PGDS in observable quantities to carry out certain cellular activities. L-PGDS not only functions to synthesize PGD₂, it can also induce glial cell migration and influence cell morphology independent of PGD₂ as discovered by Suk (2012). Considering the combined insights from Payne's study of glioma grade transition, the studies done in the Human Protein Atlas, and our findings here, one could suggest that L-PGDS possesses a more complex role in glioma development because of its absence and then sudden presence in GBMs. Further studies must be conducted to investigate if L-PGDS influences GBM apart from PGD₂ synthesis. Such studies would confirm if L-PGDS a viable target for future therapies. Our project was focused on the L-PGDS product PGD₂.

In order for PGD₂ to exert its influence on cellular activities, the necessary receptors must first be present. The next aspect investigated was confirming the presence of DP1, DP2, and TP

receptors. The DP1 receptor gene was not expressed in cell lines A-172 and T-98G. There was some weak expression observed in cell lines U-138MG, U-251MG, and U-87MG. The DP2 receptor gene was expressed in all five cell lines. The HPA, found no expression of DP1 and DP2 in the cell lines U-251MG and U-87MG which conflicts with our results (Uhlen et al., 2012). However, when our immunohistochemistry was performed, there was an unambiguous presence of DP1 and DP2 receptors. The HPA has not yet performed immunohistochemistry for these cell lines. The DP1 receptor leads to various pathways that have proven to produce anti-tumorigenic effects. Meanwhile, the DP2 receptor leads to various intracellular pathways that tend to yield pro-tumorigenic effects (Murata et al., 2008; Pettipher, 2008).

Similar to the DP2 receptor, the thromboxane A₂ receptor influences pro-tumorigenic pathways, and it is able to bind with PGD₂ (Hamid-Bloomfield et al., 1990). The TP gene was found in all five cell lines. Its presence in the U-87MG cell line has been confirmed by Giese et al. (1999). The Human Protein Atlas also found a weak expression of this receptor in U-138MG, U-251MG, and U-87MG (Uhlen et al., 2012). Our immunohistochemistry confirmed the presence of the TP receptor in U-251MG, U-87MG, and A-172. In Ekambara et al.'s review of TP function in cancer, several studies were cited confirming that TP is crucial in activating the processes of neoplastic transformation in multiple cancer types such as prostate cancer, breast cancer, lung cancer, and brain cancer (Ekambara et al., 2011). In gliomas, when thromboxane A₂ synthase was inhibited thus blocking thromboxane A₂ signaling, there was a decrease in cell migration and a decrease in intercellular adhesion (Giese et al., 1999). Results such as these suggest that future studies should directly aim at antagonizing TP and targeting its agonists for their functional roles in cancer progression (Ekambara et al., 2011).

As a point of comparison, components of the PGE₂ pathway were also investigated in these cell lines. Gene expression of mPGES1 through RT-PCR was only found in U-87MG. The HPA also found RNA expression of mPGES1 in U-87MG and no expression in U-251 MG or in U-138 MG (Uhlen et al., 2012). Payner et al. also found mPGES1 expression in U-87MG and in T-98G. However, they did not detect mPGES1 in U-138MG (Payner et al., 2006). Using immunohistochemistry, we observed a strong staining of mPGES1 in U-87MG, U-251MG and A172. The HPA also observed staining for mPGES1 in U-87MG and U-138MG (Uhlen et al.,

2012). Gathering this data from our study and the others mentioned, we have reason to believe that mPGES1 is expressed and produced in the five glioma cell lines A-172, U-251MG, U-87MG, U-138MG, and T-98G. Payner et al. (2006) demonstrated that blocking mPGES1 activity and expression inhibited the release of PGE₂ and decreased cellular proliferation. This implies that mPGES1 can regulate glioma growth through a PGE₂-dependent pathway, making mPGES1 a valuable target for treatments.

We also found the expression of the mPGES2 gene in all five cell lines. Results published by Gomes and Colquhoun have already confirmed mPGES2's presence in the T-98G cell line (Gomes and Colquhoun, 2012). The HPA observed strong RNA expression of mPGES2 in U-138MG, U-251MG, and U-87MG (Uhlen et al., 2012). Our immunohistochemistry has confirmed mPGES2 presence in A-172, U-251MG, and U-87MG. The HPA also presented positive staining for the mPGES2 protein in U-138MG, U-251MG, and U-87MG (Uhlen et al., 2012). These combined results prove that mPGES2 is produced in the five glioma cell lines investigated. According to Murakami et al., although mPGES2 is not as quickly induced during inflammation as mPGES1, it does appear to be involved in tissue homeostasis and diseases such as colorectal cancer (Murakami et al., 2003).

We found the cPGES gene expression in cell lines U-138, U-87MG and T-98G. The presence of cPGES in U-138MG, U-251MG, U-87MG and T-98G can be confirmed by the Human Protein Atlas and in Gomes and Colquhoun's study (Gomes and Colquhoun, 2012; Uhlen et al., 2012). Our immunohistochemistry confirmed the presence of this enzyme in the U-251MG cell line, as well as in A-172 and in U-87MG. Cytosolic PGE synthase seems capable of converting COX-1 derived PGH₂ to PGE₂ but not COX-2 derived PGH₂ (Tanioka et al., 2000). This enzyme, like mPGES2, is involved with tissue homeostasis. Mattila et al. discovered that the three PGE₂ synthases are all overexpressed in nearly 94 human gliomas samples (Mattila et al., 2009). These observations explain the elevated abundance of PGE₂ in U-251MG, U-87MG, and A-172 observed by our HPLC tandem mass spectrometry. The PGE₂ synthases all prove to be valuable targets of inhibition for glioma therapy.

The RT-PCR revealed that the receptors EP2 and EP4 were found in all five cell lines. EP2's presence in cell line T-98G is confirmed by Gomes and Colquhoun's study (Gomes and

Colquhoun, 2012). The Human Protein Atlas also reported a weak RNA expression of EP2 in cell lines U-138MG and U-87MG, and a weak expression of EP4 in U-251MG, U-138MG, and U-87MG. However, they found no expression of EP3 (Uhlen et al., 2012). We identified the presence of EP2 and EP4 receptors in three of our cell lines through immunohistochemistry. When Jiang and Dingledine activated EP2 it promoted prostate cancer cell growth and invasion as well as upregulating tumor-promoting inflammatory cytokines like IL-6 (Jiang and Dingledine, 2013). Also, when Kambe et al. inhibited EP4 expression, suppression in glioma cell growth was observed (Kambe et al., 2009). The presence of EP2 and EP4 is significant because it implies that even if PGD₂ is capable of anti-tumorigenic activity through its DP1 receptor, the abundance of PGE₂ could easily mask PGD₂'s impact by activating EP2 and EP4 signaling pathways. Looking to selectively block the PGE₂/EP2 and PGE₂/EP4 signaling pathways via small molecule antagonists might present a novel therapy for GBM development (Jiang and Dingledine, 2013).

Finally, our HPLC tandem mass spectrometry confirmed the existence of PGE₂ and PGD₂ in the two cell lines U-251MG and U-87MG. PGE₂ was found in A-172, but PGD₂ was below detectable quantities. Although there is a significantly higher amount of PGE₂, PGD₂ is present in detectable quantities. This difference could be due to its PGE₂'s more available synthases competing with L-PGDS for PGH₂, and PGE₂'s more chemically stable structure compared to PGD₂. Our results from the RT-PCR, the immunohistochemistry, and the tandem mass spectrometry have confirmed that the PGD₂ synthesis pathway does exist and it is functional in these cell lines of GBM.

Table 5.1. A summary of The Human Protein Atlas studies of certain proteins in glioma cell lines.

Protein Atlas Data							
	RNA Expression(FPKM: 0-100) / Protein staining (Score: 0-8000)					Location:	Stained in Glioma:
	A-172	U-138MG	U-251MG	U-87MG	T-98G		
COX-1		1 / not tested	0 / not tested	1 / not tested		Cerebral cortex- Glial cells- Medium, Neuronal cells- low. Hippocampus- Glial/Neuronal cells- medium. Lateral Ventrical- Glial cells- medium. Cerebellum- Granular layer- low, Molecular layer- medium	Not Detected
COX-2		14 / 3373	1 / 962	21 / 5546		Cerebral Cortex- Neuronal cells- low. Hippocampus- Neuronal cells- lows. Lateral Ventrical- Neuronal cells- low.	Low/Medium
LPGDS		2 / not tested	0 / not tested	0 / not tested		Cerebral Cortex- Endothelial/Neuronal cells -high. Hippocampus- Glial cells -medium, Neuronal cells- low. Cerebellum- Granular/Purkinje cells- low, Molecular layer- medium. Lateral Ventrical- Neuronal/Glial cells- low.	Medium/High
HPGDS		0	0	0		Lateral Ventrical- neuronal cells -low	Not detected
mPGES 1		strong	not tested	not tested		Cerebral Cortex- Endothelial cells- medium, Neuronal cells- low. Cerebellum- Purkinje cells- Medium	Not detected

mPGES 2		36 / 3564	42 / 3860	32 / 3582		Cerebral Cortex- Endothelial/Glial/Neuronal/Neuropil cells- medium. Hippocampus- Glial/Neuronal cells- medium. Lateral Ventricular- Glial cells- medium, Neuronal cells- medium. Cerebellum- Granular layer- medium, Molecular layer- high, Purkinje cells- low	Medium/High
cPGES		105 / not tested	185 / not tested	136 / tested		Cerebral Cortex- Neuronal cells- medium. Hippocampus- Glial/Neuronal cells- lows. Lateral Ventricular- Glial/Neuronal cells- low. Cerebellum- Granular layer/Purkinje cells- low	Low/Medium
EP1		0 / not tested	not tested	not tested		<i>not available</i>	<i>not available</i>
EP2		1 / not tested	0 / not tested	4 / not tested		<i>not available</i>	<i>not available</i>
EP3		0 / not tested	0 / not tested	0 / not tested		Cerebral Cortex- Endothelial/Neuronal cells- low	Low
EP4		5 / not tested	1 / not tested	2 / not tested		Cerebral Cortex- Endothelial cells- medium, Glial/Neuronal cells- high. Hippocampus- Glial cells- medium, Neuronal cells- high. Lateral Ventricular- Glial cells- high, Neuronal cells- low. Cerebellum- Granular/Molecular layer/Purkinje cells- high	High
DP1		0 / not tested	0 / not tested	0 / not tested		<i>not available</i>	<i>not available</i>
DP2		0 / 0	0 / 0	0 / 0		Cerebral Cortex- Neurophil- low	Not Detected
TP		3 / not tested	2 / not tested	2 / not tested		<i>not available</i>	<i>not available</i>

5.2 The Impact of PGD₂ on Cellular Activity

Since the presence of PGD₂ production and the components of its biochemical pathway have been confirmed, the next part of this study investigated PGD₂ influence on GBM's cellular activities as seen in mitosis, apoptosis, cell count of sample populations, and viability. First, we examined the cellular responses to varying concentrations of PGD₂ over 72 hours. The first set of treatments had concentrations of PGD₂ close to the highest concentration of physiological PGD₂ found in human mast cells: 0.112 μ M (Lewis et al., 1982). Treatments applied with similar concentrations and some slightly lower/higher concentrations, demonstrated very significant increases in cell count in cell lines U-251MG and A-172. The effects of PGD₂ treatment on cell count were equal to those of PGE₂ at the same concentrations in the same cell lines (see **Figures 4.4 - 4.7**). The concentration which seemed to present the most significant impact on cell count was 0.35 μ M PGD₂. It was then applied to U-251MG, U-87MG, and A-172 to evaluate its influence on their cell viability during a 72 hour period. The results showed that there was no overall impact on the viability of the cells lines studied, suggesting that this is probably not the mechanism through which physiological concentrations of PGD₂ act (see **Figures 4.11 - 4.13**).

In vitro tests performed on astrocytes of mice by Toyomoto et al., Kesslack et al. and Mizuno et al. proved that both PGE₂ and PGD₂ stimulate nerve growth factor secretion and synthesis/secretion of brain derived neurotrophic factor in the hippocampus (Kesslak et al., 1998; Mizuno et al., 2000; Toyomoto et al., 2004). This can be confirmed in the Human Protein Atlas by the presence of PGD₂ enzyme L-PGDS found amongst glial cells in the hippocampus and in other regions such as the cerebral cortex (Uhlen et al., 2012). Larjavaara's study revealed that the more likely locations to find glioblastomas are in the frontal and temporal lobes (Larjavaara et al., 2007). In glioma cell lines T-98G and U-87MG, Zhang et. al. observed significant Ca²⁺ signaling through gap junctions (Zhang et al., 2003). Significant levels of L-PGDS in regions of the brain such as those mentioned, suggest that PGD₂ influence on astrocyte communication through Ca²⁺ signaling, as observed by Mohri et al., could also apply to gliomas (Mohri et al., 2006).

After examining PGD₂ concentrations at physiological levels in three cell lines, we decided to study the impact of supraphysiological concentrations: 1 μ M, 5 μ M, and 10 μ M. The results

observed were contrary to the physiological concentrations. Although 1 μM and 5 μM PGD_2 had no significant influence on cell count, 10 μM PGD_2 significantly reduced cell count over a 72 hour period. These results are similar to the results found by Honda, who treated *in vitro* GBM with 8 μM PGD_2 (Honda and Tabuchi, 1986). Investigating a potential mechanism of action, we applied 10 μM of PGD_2 to cells to observe its effects on cell viability. There were significant decreases in cell viability in the cells lines studied. When applying this same concentration to observe its influence on apoptosis and mitosis we observed no significantly influence on apoptosis, but there was a significant decrease in cellular mitosis observed in the U-251MG cell line and a similar decrease in the A-172 cell line. This suggests that PGD_2 , at an extreme concentration such as 10 μM , may not kill cells directly, but rather it significantly impacts cellular viability and mitotic activity. In rat renal papillary tissue, PGD_2 regulates phosphatidylcholine (PC) synthesis for the preservation of cell membrane homeostasis and cell viability (Fernandez-Tome et al., 2004). It may be possible that extreme concentrations of PGD_2 produce a negative feedback on PC synthesis, thus weakening cell viability.

A review of PGD_2 / PGDS functions at nanomolar and micromolar concentrations was summarized in a table by Sandig et al. Their review showed pro-inflammatory activities generated by PGD_2 in cells of the immune system at nanomolar concentrations via the DP2 pathway. At such concentrations (1 nM, 10 nM, 100 nM PGD_2) the DP2 receptor induced Th2 cell migration, as well as IL-4, IL-5 and IL-6 production (Gervais et al., 2001; Xue et al., 2005). In addition to this, at such concentrations PGD_2 concentrations the natural response of T lymphocytes via the DP1 receptor is to inhibit interferon gamma (IFN- γ) production; IFN- γ possesses anti-tumor properties (Sandig et al., 2007; Schroder et al., 2004). Considering that human cerebral spinal fluid (CSF) contains between 0.4nM to 5.3nM PGD_2 and PGD_2 has a strong affinity for DP2, an argument could be made that PGD_2 's endogenous presence in the CSF could support GBM survival (Gaetani et al., 1986). Even though our results showed that micromolar PGD_2 had no effect on cell viability, there was a very significant increase in cell count. Micromolar concentrations of PGD_2 on GBM should be tested in other typical cellular activities such as apoptosis, mitosis, and migration in order to define its role more specifically.

Studying micromolar PGD₂ concentrations *in vivo* should also yield more interesting results due to PGD₂'s dynamic relationship with the immune response.

However, Sandig et al. also showed that PGD₂ inhibited many of the pro-inflammatory activities at micromolar concentrations ($\geq 1 \mu\text{M}$). Via the DP1 receptor, micromolar PGD₂ inhibits monocyte migration, antigen-presenting cells (APC) migration, and dendritic cell differentiation. These types of responses yield anti-inflammatory effects. Also, PGD₂'s activation of PPAR γ in nanomolar concentrations increases eosinophil migration, yet in micromolar concentrations this receptor induces lymphocyte apoptosis and inhibits lymphocyte proliferation (Sandig et al., 2007). Our treatments using 10 μM PGD₂ demonstrated a significant decrease in cell count, cell viability and mitotic activity. Although cell death was not directly induced, 10 μM PGD₂ appears to have slowed down GBM growth. It is possible that micromolar PGD₂ studied *in vivo* may produce a clearer understanding of its influence on the immunological response towards GBM and its influence on GBM susceptibility to modern treatments.

6 CONCLUSION

The objective of this study was to define the general role of PGD₂ and its influence in glioblastomas, to contribute to a solid foundation of knowledge concerning one of the more prevalent prostaglandins in the brain. The following points summarize our findings:

- Confirmation of mRNA expression and production of PGD₂ enzymes and receptors in the cell lines studied.
- Confirmation of a relationship between the concentrations of PGD₂ treatments and effects in cell count.
- Confirmation of the affects on cell count, cell viability, and mitosis caused by exogenous 10 μM PGD₂ over a 72h period.

The discovery of the opposing roles that PGD₂ possesses within a single system such as cancer development and other diseases is adding a new dimension to the study of prostaglandin function. For example, in asthma, when the receptor DP2 is activated it induces dendritic cell migration to thoracic lymph nodes thus causing an increase in antigen-specific T-Helper 2 response to the lungs. However, when the DP1 receptor is activated, dendritic cell migration is suppressed, thus inhibiting T-cell migration (Hammad et al., 2003). In transgenic mice with oil-induced dermatitis, activation of DP1 had suppressive effects in the early phase of inflammation, but DP2 is activated to promoted inflammation in a later phase (Sarashina et al., 2014). These results demonstrate that PGD₂ acting through various receptors, and as previously reviewed acting at various concentrations, can produce opposing responses within a single system. This conflict accompanied by our results suggests that although PGD₂ likely aids GBM growth and survival because of lower endogenous concentrations and strong binding affinity to DP2, there still exists the possibility that through higher concentrations and via the DP1 and PPAR γ receptors, PGD₂ could be useful in treating gliomas. PGD₂ and its metabolites have already demonstrated anti-tumorigenic qualities when treating colon cancer, colorectal cancer, acute lung carcinoma, breast cancer, leukemia, and urinary bladder carcinoma (Nakamura et al.,

2011). Future studies are needed to continue to explore the pathways influenced by PGD_2 in order to clearly define its role in GBM development.

REFERENCES*

- Aktipis C, Nesse RM. Evolutionary foundations for cancer biology. *Evol Appl.* 2013;6(1):144–59.
- Caterina DR, Basta G. N-3 Fatty acids and the inflammatory response — biological background. *European Heart Journal Supplements.* 2001;3:D42–D49.
- Ekambara P, Lambiv W, Cazzoli R, Ashton AW, Honn KV. The thromboxane synthase and receptor signaling pathway in cancer: an emerging paradigm in cancer progression and metastasis. *Cancer Metastasis Rev.* 2011;30(0):397–408.
- Ferlay J, Soerjomataram I, Ervik M, Dikshit R, Eser S, Mathers C, Rebelo M, Parkin DM, Forman D, Bray F. International Agency for Research on Cancer. [Internet]. GLOBOCAN 2012 Cancer Incidence and Mortality Worldwide: IARC CancerBase. [Updated 10 dec 2013]. Available from: <http://globocan.iarc.fr>.
- Fernández-Tome M1, Kraemer L, Federman SC, Favale N, Speziale E, Sterin-Speziale N. COX-2-mediated PGD2 synthesis regulates phosphatidylcholine biosynthesis in rat renal papillary tissue. *Biochem Pharmacol.* 2004;67(2):245-54.
- Fisher PG, Tihan T, Goldthwaite PT, Wharam MD, Carson BS, Weingart JD, Repka MX, Cohen KJ, Burger PC. Outcome analysis of childhood low-grade astrocytomas. *Pediatr Blood Cancer.* 2008;51:245–50.
- Gaetani P, Silvani V, Crivellari MT, Viganò T, Rodriguez y Baena R, Paoletti P. Prostaglandin D2 monitoring in human CSF after subarachnoid hemorrhage: the possible role of prostaglandin D2 in the genesis of cerebral vasospasm. *Ital J Neurol Sci.* 1986;7(1):81-8.
- Gervais FG, Cruz RP, Chateauneuf A, Gale S, Sawyer N, Nantel F, Metters KM, O'Neill GP. Selective modulation of chemokinesis, degranulation, and apoptosis in eosinophils through the PGD2 receptors CRTH2 and DP. *J Allergy Clin Immunol.* 2001;108(6):982-8.
- Giese A, Hagel C, Kim EL, Zapf S, Djawaheri J, Berens ME, Westphal M. Thromboxane synthase regulates the migratory phenotype of human glioma cells. *Neuro Oncol.* 1999;1:3–13.
- Gomes RN, Colquhoun A. E series prostaglandins alter the proliferative, apoptotic and migratory properties of T98G human glioma cells in vitro. *Lipids Health Dis.* 2012;11:171.

* In accordance with:

International Committee of Medical Journal Editors. [Internet]. Uniform requirements for manuscripts submitted to Biomedical Journal: sample references. [updated 2011 Jul 15]. Available from: <http://www.icmje.org>

Grange JM, Stanford JL, Stanford CA. Campbell De Morgan's 'Observations on cancer', and their relevance today. *J R Soc Med.* 2002;95(6):296–9.

Greenberg MS. Astrocytoma. In: *Handbook of Neurosurgery.* Greenberg Graphics Inc. 1997;4(1):244-56.

Hamid-Bloomfield S, Payne AN, Petrovic AA, Whittle BJR. The role of prostanoid TP- and DP-receptors in the bronchoconstrictor effect of inhaled PGD₂ in anaesthetized guinea-pigs: effect of the DP-antagonist BW A868C. *Br J Pharmacol.* 1990;100:761-6.

Hammad H, de Heer HJ, Soullie T, Hoogsteden HC, Trottein F, Lambrecht BN. Prostaglandin D₂ inhibits airway dendritic cell migration and function in steady state conditions by selective activation of the D prostanoid receptor 1. *J Immunol.* 2003;171:3936–40.

Hanahan D, Weinberg RA. Hallmarks of cancer: the next generation. *Cell.* 2011;144(5):646-74.

Harris SG, Padilla J, Koumas L, Ray D, Phipps RP. Prostaglandins as modulators of immunity. *Trends Immunol.* 2002;23(3):144-50.

Honda C, Tabuchi K. Effects of prostaglandin D₂ on cultured glioma cells. *Gan To Kagaku Ryoho.* 1986;13(9):2758-65.

Hwang SL, Lee KS, Lin CL, Lieu AS, Cheng CY, Loh JK, Hwang YF, Su YF, Howng SL. Effect of aspirin and indomethacin on prostaglandin E₂ synthesis in C6 glioma cells. *Kaohsiung J Med Sci.* 2004;20(1):1-5.

Jakobsson P J, Engblom D, Ericsson-Dahlstrand A, Blomqvist A. Microsomal Prostaglandin E Synthase: A Key Enzyme in PGE₂ Biosynthesis and Inflammation. *Current Medicinal Chemistry - Anti-Inflammatory & Anti-Allergy Agents.* 2002;1(3):167-75.

Jemal A, Bray F, Center MM, Ferlay J, Ward E, Forman D. Global cancer statistics. *CA: A Cancer Journal for Clinicians.* 2011;61(2):69–90.

Jiang J, Dingledine R. Role of prostaglandin receptor EP₂ in the regulations of cancer cell proliferation, invasion, and inflammation. *J Pharmacol Exp Ther.* 2013;344(2):360-7.

Joo M, Sadikot RT. PGD Synthase and PGD₂ in Immune Response. *Mediators of Inflammation.* 2012;2012:1-6.

Kambe A, Yoshioka H, Kamitani H, Watanabe T, Baek SJ, Eling TE. The cyclooxygenase inhibitor sulindac sulfide inhibits EP₄ expression and suppresses the growth of glioblastoma cells. *Cancer Prev Res (Phila).* 2009;2(12):1088-99.

Keenan CM, Rangachari PK. Contrasting effects of PGE2 and PGD2: ion transport in the canine proximal colon. *Am J Physiol Gastrointest Liver Physiol*. 1991;260(3):G481-8.

Kesslak JP, So V, Choi J, Cotman CW, Pinilla FG. Learning upregulates brain-derived neurotrophic factor messenger ribonucleic acid: a mechanism to facilitate encoding and circuit maintenance? *Behav Neurosci*. 1998;112:1012-9.

Kiriyama M, Ushikubi F, Kobayashi T, Hirata M, Sugimoto Y, Narumiya S. Ligand binding specificities of the eight types and subtypes of the mouse prostanoid receptors expressed in Chinese hamster ovary cells. *British Journal of Pharmacology*. 1997;122: 217-24.

Kostenis E, Ulven T. Emerging roles of DP and CRTH2 in allergic inflammation. *Trends Mol Med*. 2006;12(4):148-58.

Larjavaara S, Mäntylä R, Salminen T, Haapasalo H, Raitanen J, Jääskeläinen J, Auvinen A. Incidence of gliomas by anatomic location. *Neuro Oncol*. 2007;9(3):319–25.

Lee S, Jang E, Kim J, Kim JH, Lee W, Suk K. Lipocalin-type Prostaglandin D2 Synthase Protein Regulates Glial Cell Migration and Morphology through Myristoylated Alanine-rich C-Kinase Substrate. *J Biol Chem*. 2012;287: 9414-28.

Lewis RA, Soter NA, Diamond PT, Austen KF, Oates JA, Roberts LJ 2nd. Prostaglandin D2 generation after activation of rat and human mast cells with anti-IgE. *J Immunol*. 1982;129(4):1627-31.

Louis DN, Ohgaki H, Wiestler OD, Cavenee WK, Burger PC, Jouvett A, Scheithauer BW, Kleihues P. The 2007 WHO classification of tumours of the central nervous system. *Acta Neuropathol*. 2007;114(2):97-109.

Luzheng Xue, Shân L. Gyles¹, Frank R. Wetthey, Lucien Gazi³, Elizabeth Townsend, Michael G. Hunter and Roy Pettipher. Prostaglandin D2 Causes Preferential Induction of Proinflammatory Th2 Cytokine Production through an Action on Chemoattractant Receptor-Like Molecule Expressed on Th2 Cells. *The Journal of Immunology*. 2005;175(10):6531-6.

Mattila S, Tuominen H, Koivukangas J, Stenbäck F. The terminal prostaglandin synthases mPGES-1, mPGES-2, and cPGES are all overexpressed in human gliomas. *Neuropathology*. 2009;29(2):156-65.

Mizuno M, Yamada K, Olariu A, Nawa H, Nabeshima T. Involvement of brain-derived neurotrophic factor in spatial memory formation and maintenance in a radial arm maze test in rats. *J Neurosci*. 2000;20:7116-21.

Mohri I, Taniike M, Taniguchi H, Kanekiyo T, Aritake K, Inui T, Fukumoto N, Eguchi N, Kushi A, Sasai H, Kanaoka Y, Ozono K, Narumiya S, Suzuki K, Urade Y. Prostaglandin D2-mediated

microglia/astrocyte interaction enhances astrogliosis and demyelination in twitcher. *J Neurosci.* 2006;26(16):4383-93.

Murakami M, Nakashima K, Kamei D, Masuda S, Ishikawa Y, Ishii T, Ohmiya Y, Watanabe K, Kudo I. Cellular Prostaglandin E₂ Production by Membrane-bound Prostaglandin E Synthase-2 via Both Cyclooxygenases-1 and -2. *J Biol Chem.* 2003;278(39):37937-47.

Murata T, Aritakeb K, Matsumotoa S, Kamauchib S, Nakagawac T, Horia M, Momotanid E, Uradeb Y, Ozaki H. Prostaglandin D₂ is a mast cell-derived antiangiogenic factor in lung carcinoma. *PNAS.* 2011;108(49):19802–7.

Murata T, Linb MI, Aritakec K, Matsumotoa S, Narumiyad S, Ozakia H, Urade Y, Horia M, Sessab WC. Role of prostaglandin D₂ receptor DP as a suppressor of tumor hyperpermeability and angiogenesis in vivo. *Proc Natl Acad Sci U S A.* 2008;105(50):20009-14.

Murata T, Aritake K, Tsubosaka Y, Maruyama T, Nakagawa T, Hori M, Hirai H, Nakamura M, Narumiya S, Urade Y, Ozaki H. Anti-inflammatory role of PGD₂ in acute lung inflammation and therapeutic application of its signal enhancement. *Proc Natl Acad Sci U S A.* 2013;110(13):5205-10.

Nakamura M, Yamaguchi S, Motoyoshi K, Negishi M, Taki TS, Matsumoto K, Hayashi I, Majima M, Kitasato H. Anti-tumor effects of prostaglandin D₂ and its metabolites, 15-deoxy- Δ 12, 14-PGJ₂, by peroxisome proliferator-activated receptor (PPAR) γ -dependent and -independent pathways. *Inflammation and Regeneration.* 2011;31(2):189-95.

Nakanishi M, Montrose DC, Clark P, Nambiar PR, Belinsky GS, Claffey KP, Xu D, Rosenberg DW. Genetic deletion of mPGES-1 suppresses intestinal tumorigenesis. *Cancer Res.* 2008;68:3251–9.

Nakatani Y, Hokonohara Y, Tajima Y, Kudo I, Hara S. Involvement of the constitutive prostaglandin E synthase cPGES/p23 in expression of an initial prostaglandin E₂ inactivating enzyme, 15-PGDH. *Prostaglandins Other Lipid Mediat.* 2011;94(3-4):112-7.

Nathoo N, Barnett GH, Golubic M. The eicosanoid cascade: possible role in gliomas and meningiomas. *J Clin Pathol.* 2004;57:6-13.

Ohgaki H, Kleihues P. The definition of primary and secondary glioblastoma. *Clin Cancer Res.* 2013;19(4):764-72.

Otero J, David Rowitch,² and Scott Vandenberg. OLIG2 is differentially expressed in pediatric astrocytic and in ependymal neoplasms. *J Neurooncol.* 2011;104(2):423–438.

Parpura V, Heneka MT, Montana V, Oliekt SHR, Schousboe A, Haydon PG, Stout RF, Spray DC, Reichenbach A, Pannicke T, Pekny M, Pekna M, Zorec R, Verkhratsky A. Glial cells in (patho)physiology. *J Neurochem.* 2012;121(1): 4–27.

Payne CA, Sanaz M, Messina M, O'Sullivan MG, Stone G, Hall NR, Parkinson JF, Wheeler HR, Cook RJ, Biggs MT, Little NS, Teo C, Robinson BG, McDonald KL. Loss of prostaglandin D2 synthase: a key molecular event in the transition of a low-grade astrocytoma to an anaplastic astrocytoma. *Mol Cancer Ther.* 2008;7(10):3420–8.

Payner T, Leaver HA, Knapp B, Whittle IR, Trifan OC, Miller S, Rizzo MT. Microsomal prostaglandin E synthase-1 regulates human glioma cell growth via prostaglandin E2-dependent activation of type II protein kinase A. *Mol Cancer Ther.* 2006;5:1817.

Pettipher R, Hansel TT, Armer R. Antagonism of the prostaglandin D2 receptors DP1 and CRTH2 as an approach to treat allergic diseases. *Nature Reviews Drug Discovery.* 2007;6(4):313–25.

Pettipher R. The roles of the prostaglandin D2 receptors DP1 and CRTH2 in promoting allergic responses. *Brit J Pharmac.* 2008;153:S191-9.

Pfrieger FW. Roles of glial cells in synapse development. *Cell Mol Life Sci.* 2009;66(13): 2037–47.

Pinzar E, Miyano M, Kanaoka Y, Urade Y, Hayaishi O. Structural Basis of Hematopoietic Prostaglandin D Synthase Activity Elucidated by Site-directed Mutagenesis. *J of Bio Chem.* 2000;275(40):31239–44.

Ram A, Pandey HP, Matsumura H, Kasahara-Orita K, Nakajima T, Takahata R, Satoh S, Terao A, Hayaishi O. CSF levels of prostaglandins, especially the level of prostaglandin D2, are correlated with increasing propensity towards sleep in rats. *Brain Res.* 1997;751(1):81-9.

Rao S, Srinivasan S, Patric IRP, Hegde AS, Chandramouli BA, Arimappamagan A, Santosh V, Kondaiah P, Rao MRS, Somasundaram K. A 16-Gene Signature Distinguishes Anaplastic Astrocytoma from Glioblastoma. *PLoS One.* 2014;9(1):e85200.

Rodriguez FJ, Lim KS, Bowers D, Eberhart CG. Pathological and Molecular Advances in Pediatric Low Grade Astrocytoma. *Annu Rev Pathol.* 2013;8:361–79.

Rundhaug JE, Simper MS, Surh I, Fischer SM. The role of the EP receptors for prostaglandin E2 in skin and skin cancer. *Cancer Metastasis Rev.* 2011;30:465–80.

Sandig H, Pease JE, Sabroe I. Contrary prostaglandins: the opposing roles of PGD2 and its metabolites in leukocyte function. *J Leukocyte Bio.* 2007;81:372-82.

Sang N, Zhang J, Chen C. PGE2 glycerol ester, a COX-2 oxidative metabolite of 2-arachidonoyl glycerol, modulates inhibitory synaptic transmission in mouse hippocampal neurons. *J Physiol.* 2006;572(3):735–45.

Sarashina H, Tsubosaka Y, Omori K, Aritake K, Nakagawa T, Hori M, Hirai H, Nakamura M, Narumiya S, Urade Y, Ozaki H, Murata T. Opposing Immunomodulatory Roles of Prostaglandin D2 during the Progression of Skin Inflammation. *J Immunol.* 2014;192(1):459-65.

Sassi Y, Lipskaia L, Vandecasteele G, Nikolaev VO, Hatem SN, Aubart FC, Russel FG, Mougnot N, Vrignaud C, Lechat P, Lompré A, Hulotet JS. Multidrug resistance-associated protein 4 regulates cAMP-dependent signaling pathways and controls human and rat SMC proliferation. *J Clin Invest.* 2008;118(8):2747-57.

Sawamura Y, Diserens AC, Tribolet N. In vitro Prostaglandin E2 production by glioblastoma cells and its effect on interleukin-2 activation of oncolytic lymphocytes. *Journal of Neuro-Oncology.* 1990;9(2):125-30.

Sawyer N, Cauchon E, Chateauneuf A, Cruz RP, Nicholson DW, Metters KM, O'Neill GP, Gervais FG. Molecular pharmacology of the human prostaglandin D2 receptor, CRTH2. *Br J Pharmacol.* 2002;137(8):1163-72.

Schmidt NO, Ziu M, Cargioli T, Westphal M, Giese A, Black PM, Carroll RS. Inhibition of Thromboxane Synthase Activity Improves Glioblastoma Response to Alkylation Chemotherapy¹. *Translational Oncology.* 2010;3:43-9.

Schroder K, Hertzog PJ, Ravasi T, Hume DA. Interferon-gamma: an overview of signals, mechanisms and functions. *J Leukoc Biol.* 2004;75(2):163-89.

Suk K. Unexpected role of lipocalin-type prostaglandin D synthase in brain regulation of glial cell migration and morphology. *Cell Adhesion & Migration.* 2012;6(3):160-3.

Tanioka T, Nakatani Y, Semmyo N, Murakami M, Kudo I. Molecular identification of cytosolic prostaglandin E2 synthase that is functionally coupled with cyclooxygenase-1 in immediate prostaglandin E2 biosynthesis. *J Biol Chem.* 2000;275(42):32775-82.

Tassoni D, Kaur G, Weisinger RS, Sinclair AJ. The role of eicosanoids in the brain. *Asia Pac J Clin Nutr.* 2008;17(S1):220-8.

Tiberiu M, Das S. The 2-Series Eicosanoids in Cancer: Future Targets for Glioma Therapy? *Journal of Cancer Therapy.* 2013;4:338-52.

Toyomoto M, Ohta M, Okumura K, Yano H, Matsumoto K, Inoue S, Hayashi K, Ikeda K. Prostaglandins are powerful inducers of NGF and BDNF production in mouse astrocyte cultures. *FEBS Lett.* 2004;562(1-3):211-5.

Uhlen M, Oksvold P, Fagerberg L, Lundberg E, Jonasson K, Forsberg M, Zwahlen M, Kampf C, Wester K, Hober S, Wernerus H, Björling L, Ponten F. Towards a knowledge-based Human Protein Atlas. *Nat Biotechnol.* 2010;28(12):1248-50.

Vauleon E, Avril T, Collet B, Mosser J, Quillien V. Overview of cellular immunotherapy for patients with glioblastoma. *Clinical and Developmental Immunology.* 2010:18.

Wang D, DuBois RN. Eicosanoids and Cancer. *Nat Rev Cancer.* 2010;10(3):181–93.

Yamamoto Y, Takase K, Kishino J, Fujita M, Okamura N. Proteomic Identification of Protein Targets for 15-Deoxy-D12,14-Prostaglandin J2 in Neuronal Plasma Membrane. *PLoS One.* 2011;6(3):e17552.

Yoshida T, Ohki S, Kanazawa M, Mizunuma H, Kikuchi Y, Satoh H, Andoh Y, Tsuchiya A, Abe R. Inhibitory Effects of Prostaglandin D2 Against the Proliferation of Human Colon Cancer Cell Lines and Hepatic Metastasis from Colorectal Cancer. *Jpn J Surg.* 199;28:740–5.

Youdim KA, Martin A, Joseph JA. Essential fatty acids and the brain: possible health implications. *Int J Devl Neuroscience.* 2000;18:383-99.

Zeitler J M. Control of sleep and wakefulness in health and disease. *Prog Mol Biol Transl Sci.* 2013;119:137-54.

Zhang W, DeMattia JA, Song H, Couldwell WT. Communication between malignant glioma cells and vascular endothelial cells through gap junctions. *J Neurosurg.* 2003;98(4):846-53.